

Studying Systemic Metabolic Remodeling and Abnormal Mitochondrial Signaling in Primary  
Biliary Cholangitis

by

Ning Sun

A thesis submitted in partial fulfillment of the requirements for the degree of

Master of Science

Department of Medicine  
University of Alberta

© Ning Sun, 2024

## Abstract

Primary biliary cholangitis (PBC) is linked with the production of anti-mitochondrial antibodies (AMA) targeting pyruvate dehydrogenase complex-E2 subunit (PDC-E2). Cholangiocytes from PBC patients express increased PDC-E2, which is thought to result in loss of tolerance to mitochondrial proteins. We have previously shown that a human betaretrovirus resembling mouse mammary tumor virus (MMTV), leads to increased expression of PDC-E2 in cholangiocytes. To better understand these changes, we have studied the metabolism in PBC cholangiocytes and found evidence of increased glycolysis linked with altered mitochondrial function, as well as increased mitochondrial DNA and proteins in cholangiocytes from patients with PBC.

Herein, we addressed the hypothesis that a glycolytic-shift and metabolic remodeling occurs systemically both in cholangiocytes and the peripheral blood of PBC, which in turn leads to an increased PDC-E2 expression linked with mitochondrial biogenesis. We first used immunofluorescence to investigate whether HIF1  $\alpha$  pathway activation was involved in metabolic remodeling of cholangiocytes. Then, we used RNA-seq to compare transcriptomic changes in PBC patients' whole blood versus healthy controls to gain a wider perspective of the systemic changes in PBC patients' metabolism. Specifically, we focused on evaluating the mitochondrial-DNA replication and mitochondrial function by using quantitative PCR, flow cytometry, and immunocytochemistry.

We found specific biliary epithelium cells from PBC patients' were characterized with activated HIF1  $\alpha$  signaling that was not observed in other liver diseases. We also found that the peripheral blood of PBC showed increased glycolytic metabolism with an upregulated mitochondrial encoded

OXPPOS gene expression and a downregulated nuclear encoded gene expression as compared to healthy subjects. These changes of gene expression were accompanied by increased mt-DNA replication and hyperpolarized mitochondria in PBC peripheral blood. Finally, the overexpression of the mitochondrial autoantigen PDC-E2 was predominantly observed with hyperpolarized mitochondria in PBMC of patients with PBC. These findings support the hypothesis that the abnormal mitochondrial signalling characterized by hyperpolarized mitochondria induces a compensatory mitochondrial biogenesis linked with the overexpression of mitochondrial autoantigens in PBC.

## Preface

This thesis is my original work. No part of this thesis has been previously published.

All of the whole blood and PBMC used in this research was processed and isolated by Hussain Syed, Hiatem Abofayed, Bruna Dutra, Kiandokht Bashir, Cassady Lacoursiere and me. I performed the immunohistochemistry and immunofluorescence on the paraffine embedded liver tissues, took images and completed the statistical analysis. Hussain Syed and I performed the transcript's differential expression analysis of the PBMC RNA sequencing data and made the graphs showing the changes of mitochondrial encoded genes and nuclear encoded genes. I made the graph of the differential gene expressions of glycolysis pathway. I also extracted the DNA of peripheral blood of the healthy controls. The whole blood DNA samples of patients with PBC were provided by Intercept Pharma. I performed the qPCR to evaluate the mitochondrial DNA copy number of PBC and healthy controls, and completed the statistical analysis. I also performed the evaluation of the mitochondrial membrane potential in PBMC by flow cytometry, assessed the immunocytochemistry of AMA reactivity of PBMC, and sorted the TMRM-high cells and TMRM-low cells by fluorescence-activated cell sorting, and completed the statistical analysis.

This study was approved by the University of Alberta, Research Ethics Committee (Pro00005105)

## **Acknowledgement**

First and foremost, I would like to express my heartfelt gratitude to my supervisor, Dr. Andrew Mason, for his guidance, encouragement, and patience. I have learned so much from him, and I appreciate all the support he has given me.

I also warmly appreciate the help of my committee members, Dr. Mohamed Osman and Dr. Gopinath Sutendra. Their insights and guidance have greatly enriched my training as a master's student.

I am deeply thankful for having the opportunity to work with all the amazing lab members of the Mason lab, including Hussain Syed, Dr. Olaide Oyegbami, Dr. Doaa Waly, Seyed Sajjad Zadian, Varinder Madhav, Abdiel Castillo Gurdian, Glenn Ford, Dr. Georgina MacIntyre, Cassady Lacoursiere, Dr. Hiatem Abofayed, Dr. Kiandokht Bashir, Bruna Dutra, and Dr. Steven Willows. I also would like to thank Naomi Hotte who provided many helps in both research and lab experiences.

I would also like to thank the members of the Michelakis lab for welcoming me into their lab space. I must extend extra thanks to Alois Haromy, who was kind enough to help me with the confocal photomicrographs. I'd like to thank Charmaine van Eeden from the Osman lab, for her help with sharing the TMRM assay protocol and for her advice about my experiment design. And many thanks to Sudip Subedi, Aja Rieger, Lai Xu and Rikus Niemand for assisting with my experiments.

Last but not least, I would like to thank my family my husband Yongneng Zhang for his support, my kids who are my endless fountain of joy, and my parents for their unwavering support.

## Table of Contents

<i>Abstract</i> .....	<i>ii</i>
<i>Preface</i> .....	<i>iv</i>
<i>Acknowledgement</i> .....	<i>v</i>
<i>List of Figures</i> .....	<i>ix</i>
<i>List of Abbreviations</i> .....	<i>xi</i>
<b>Chapter 1: Introduction</b> .....	<b>1</b>
<b>1.1 Primary Biliary Cholangitis</b> .....	<b>1</b>
<b>1.2 PBC and autoimmunity</b> .....	<b>3</b>
<b>1.3 Environmental disease triggers</b> .....	<b>4</b>
<b>1.4 Genetic factors</b> .....	<b>5</b>
<b>1.5 Interplay between cholangiocytes and immune cells</b> .....	<b>6</b>
<b>1.6 Metabolic dysregulation and mitochondrial dysfunction in PBC cholangiocytes</b> .....	<b>10</b>
<b>1.7 Hypoxia-inducible factor 1<math>\alpha</math> (HIF1<math>\alpha</math>)</b> .....	<b>15</b>
<b>1.8 Hypothesis</b> .....	<b>16</b>
<b>1.9 Implications and importance of investigation</b> .....	<b>17</b>
<b>Chapter 2: Materials and Methods</b> .....	<b>18</b>
<b>2.1 Detections of Enolase 1 and PDC-E2 in liver tissue by immunohistochemistry</b> .....	<b>18</b>
<b>2.2 Detections of HIF1<math>\alpha</math>, PDC-E2 and CK19 in liver tissues by immunofluorescence</b> ....	<b>18</b>

<b>2.3 Visualization analysis of whole blood RNAseq data .....</b>	<b>19</b>
2.3.1 Differential gene expression analysis .....	19
2.3.2 Visualization analysis of genes in glycolysis, TCA cycle, ETC and OXPHOS .....	20
<b>2.4 Mitochondrial DNA quantitative PCR.....</b>	<b>20</b>
2.4.1 DNA extraction .....	20
2.4.2 qPCR for mtDNA copy number.....	21
<b>2.5 Evaluation of mitochondrial membrane potential in PBMC.....</b>	<b>22</b>
<b>2.6 Evaluation of AMA reactivity in PBMC by immunocytochemistry.....</b>	<b>23</b>
<b>2.7 Fluorescence-activated cell sorting.....</b>	<b>23</b>
<b>2.8 Statistical analysis .....</b>	<b>24</b>
<b><i>Chapter 3: Results.....</i></b>	<b>25</b>
<b>Section 1: Study of metabolic remodeling in PBC cholangiocytes .....</b>	<b>25</b>
3.1 Increased glycolytic enzyme expression in PBC cholangiocytes.....	25
3.2 HIF1 $\alpha$ was activated in occasional PBC cholangiocytes.....	26
<b>Section 2: Study of metabolic remodeling in PBC peripheral blood.....</b>	<b>29</b>
3.3 Dysregulated transcription of whole blood in glycolysis and the tricarboxylic acid cycle genes in PBC .....	30
3.4 Inconsistent transcription levels changes of genes in electron transport chain and oxidative phosphorylation in the whole blood of PBC .....	32
3.5 Elevated mitochondrial DNA copy number in PBC peripheral blood.....	35

<b>3.6 Elevated mitochondrial membrane potential in PBC PBMC.....</b>	<b>37</b>
<b>3.7 Increased AMA reactivity in PBC PBMC.....</b>	<b>38</b>
<b><i>Chapter 4: Discussion.....</i></b>	<b>42</b>
<b>4.1 Introduction.....</b>	<b>42</b>
<b>4.2 HIF-1 <math>\alpha</math> signaling activation .....</b>	<b>42</b>
<b>4.3 Mitochondrial phenotype in PBMC .....</b>	<b>44</b>
<b>4.4 Future directions and conclusion.....</b>	<b>47</b>

## List of Figures

<b>Figure 1. Immunohistochemistry studies show viral capsid protein in PBC patient's peri-portal lymph nodes in the same distribution as aberrant autoantigen expression .....</b>	<b>8</b>
<b>Figure 2. Normal BEC develop the phenotypic manifestation of PBC when incubated with PBC patient's lymph node homogenates .....</b>	<b>9</b>
<b>Figure 3. Normal BEC develops the phenotypic manifestation of PBC when incubated with PBC patient's lymph node homogenates .....</b>	<b>11</b>
<b>Figure 4. Cultured biliary epithelial cells (BEC) from patients with Primary Biliary Cholangitis (PBC) show elevated levels of intracellular and excreted lactate in <sup>13</sup>C glucose tracer studies .....</b>	<b>12</b>
<b>Figure 5. Intracellular levels of amino acids detected by <sup>1</sup>H NMR of cultured biliary epithelial cells (BEC) from patients with Primary Biliary Cholangitis (PBC).....</b>	<b>13</b>
<b>Figure 6. Significantly increased levels of extracellular acidification rate (ECAR) and trend for elevated oxygen consumption rate (OCR) in Primary Biliary Cholangitis (PBC) patients' biliary epithelial cells (BEC).....</b>	<b>14</b>
<b>Figure 7. Significantly higher levels of mitochondrial DNA (Mt-DNA) copy number in Primary Biliary Cholangitis (PBC) patients' biliary epithelial cells (BEC) .....</b>	<b>15</b>
<b>Figure 8. Increased glycolytic protein expression in PBC cholangiocytes .....</b>	<b>26</b>
<b>Figure 9. Activated HIF1<math>\alpha</math> signaling shown in occasional cholangiocytes in PBC .....</b>	<b>27</b>
<b>Figure 10. Double nuclei shown in the cells with activated HIF1<math>\alpha</math> signaling in PBC.....</b>	<b>29</b>
<b>Figure 11. Pathway map highlighting differentially expressed genes involved in cellular energy metabolism in PBC whole blood RNAseq analysis .....</b>	<b>31</b>

<b>Figure 12. Abnormal gene expressions of ETC and OXPHOS characterized by upregulated expressions of mitochondrial encoded genes and downregulated nuclear encoded genes in PBC whole blood RNAseq analysis .....</b>	<b>34</b>
<b>Figure 13. Mitochondrial DNA copy number is increased in PBC peripheral blood .....</b>	<b>36</b>
<b>Figure 14. Flow analysis of mitochondrial membrane potential in PBC PBMC .....</b>	<b>38</b>
<b>Figure 15. Increased AMA reactivity in PBMC of patients with PBC .....</b>	<b>39</b>
<b>Figure 16. Sorted PBMC of PBC with high TMRM have more AMA reactivity .....</b>	<b>41</b>
<b>Figure 17. The schematic of metabolism and abnormal mitochondrial signaling in cholangiocytes of patients with PBC .....</b>	<b>48</b>
<b>Figure 18. The predicted schematic of mitochondrial energy production in cholangiocytes of patients with PBC .....</b>	<b>49</b>

## List of Abbreviations

Abbreviation	Meaning
2-OADC	2-oxoacid dehydrogenase complexes
$\Delta\Psi_m$	Mitochondrial membrane potential
ALDOA	Aldolase A
ALP	Alkaline Phosphatase
AMA	Anti-mitochondrial antibody
ANA	Antinuclear antibodies
AOD	Average optical density
ATP	Adenosine triphosphate
B2M	Beta-2-microglobulin
BCA	Bicinchoninic acid assay
BCKDH	Branched chain 2-oxoacid dehydrogenase complex
BEC	Biliary epithelial cells
BLB	Bilirubin
BSA	Bovine serum albumin
CCCP	Carbonyl Cyanide m-Chlorophenylhydrazone
CK19	Cytokeratin 19
$C_t$	Cycle threshold
Crypto	Cryptogenic Cirrhosis
ECAR	Extracellular acidification rate
E. coli	Escherichia coli
EDTA	Ethylenediaminetetraacetic acid
ENO1	Enolase 1 (Alpha)
ENO2	Enolase 2 (Gamma, Neuronal)
ETC	Electron Transport Chain
FACS	Fluorescence-Activated Cell Sorting
FXR	Farnesoid X receptor
GAPDH	Glyceraldehyde 3-phosphate dehydrogenase
GPI	Glucose-6-phosphate isomerase

GWAS	Genome wide association studies
HBRV	Human betaretrovirus
HCV	Hepatitis-C virus
HIF1 $\alpha$	Hypoxia-inducible factor 1 alpha
HIV	Human immunodeficiency virus
HK	Hexokinase
HLA	Human leukocyte antigen
IF	Immunofluorescence
IFN- $\gamma$	Interferon-gamma
IHC	Immunohistochemistry
IL	Interleukin
JAK	Janus kinase
KEGG	Kyoto Encyclopedia of Genes and Genomes
LDHA	Lactate dehydrogenase
LN	Lymph node
LTR	Long Terminal Repeat
MMTV	Mouse mammary tumour virus
MFI	Median of fluorescence intensity
MHC	Major histocompatibility complex
MHP	Mitochondrial hyperpolarization
MPC	Mitochondrial pyruvate carrier
Mt-DNA	Mitochondrial DNA
MT-genes	Mitochondrial-encoded genes
NASH	Non-Alcoholic Steatohepatitis
NC-genes	Nuclear-encoded genes
NK cells	Natural Killer cells
OCA	Obeticholic Acid
OCR	Oxygen consumption rate
OGDHC	2-oxoglutarate dehydrogenase complex
OXPHOS	Oxidative phosphorylation
PBC	Primary biliary cholangitis

PBMC	Peripheral blood mononuclear cells
PBS	Phosphate buffered saline
PBST	Phosphate buffer saline supplemented with tween 20
PCR	Polymerase chain reaction
PDC	Pyruvate dehydrogenase complex
PDC-E2	E2 subunit of the pyruvate dehydrogenase complex
PDK	Pyruvate Dehydrogenase complex
PFK	Phosphofructokinase
PKM	Pyruvate kinase
PSC	Primary sclerosing cholangitis
QC	Quality control
RT-PCR	Real time PCR
qPCR	Quantitative PCR
ROS	Reactive oxygen species
SDH	Succinate dehydrogenase
SE	Standard error of the mean
STAT	Signal transducer and activator of transcription
STRING	Search Tool for the Retrieval of Interacting Genes/Proteins
TCA	Tricarboxylic Acid Cycle
TCR	T-cell receptor
TMRM	Tetramethylrhodamine Methyl Ester
TNF	Tumour necrosis factor
TPM	Transcripts Per Million
UDCA	Ursodeoxycholic acid
ULN	Upper Limit of Normal
UTI	Upper tract infection
VHL	von Hippel-Lindau

## Chapter 1: Introduction

### 1.1 Primary Biliary Cholangitis

Primary biliary cholangitis (PBC) is a chronic liver disease characterized by the progressive destruction of small intrahepatic bile ducts, leading to cholestasis. Over time, this damage can result in fibrosis and potentially progress to cirrhosis, with the associated complications (1, 2). PBC predominantly affects middle-aged females (40-60 years old), even though it is diagnosed in all sexes and races (3), with the prevalence and incidence increasing fivefold and fourfold, respectively, in women more so than men in European and Asian countries (3, 4). The reasons behind this are not yet fully understood. However, male patients and young patients tend to be diagnosed at more advanced stages of the disease and experience an increased mortality (4, 5). It is thought that the improved awareness of the disease has resulted a greater proportion of patients diagnosed at an earlier stage of disease and this has led to an increased incidence and prevalence of PBC in recent decades (6, 7). The estimated global incidence and prevalence of PBC are 1.76 and 14.6 per 100,000 persons, respectively (3, 6). The prevalence in North American and Sweden, which has increased to 1:3,000, is higher than that in the Asia-Pacific region (7).

Most patients are asymptomatic at diagnosis, then will develop symptoms within two decades (8). Fatigue is the most common symptom, affecting up to 85% of patients, and has been identified as one of the major determinants affecting patients' quality of life and well-being. Other symptoms include pruritus, jaundice, xanthomas and xanthelasmas, abdominal pain, and dry eyes and mouth (9).

The criteria for diagnosis are elevated alkaline phosphatase with the production of anti-mitochondrial antibody (AMA) in serum. For patients without AMA, other criteria are histological changes including florid duct lesions, periportal inflammation and progressive fibrosis and cirrhosis shown by liver biopsy (10).

At present, we lack curative therapies due to the unknown etiology and mechanisms that drive disease. Ursodeoxycholic acid (UDCA) is the first line therapy, which decreases biochemical values and delays the progression and complication of PBC but has no effect on symptoms (11). The transplant-free survival rates are 79.7% and 60.7% in UDCA treated patients and untreated patients, respectively (12). However, not all patients benefit from UDCA treatment. Alkaline phosphatase (ALP) levels are considered an independent effective marker of prognosis and treatment response. If the ALP levels remain greater than 2x ULN after 1 year UDCA treatment, patients are considered incomplete responders (13). Patients with poor biochemical response to UDCA have a high risk of developing complications.

The potent farnesoid X receptor (FXR) agonist, obeticholic acid (OCA), is considered a second-line therapy following the demonstration that 46% of patients unresponsive to UDCA achieved the composite endpoints of improved hepatic biochemistry as the POISE criteria (serum ALP reduction to  $<1.67 \times$  ULN, with a reduction of at least 15% from baseline and a normal total bilirubin level after 12 months of treatment) (14). Liver transplantation is the treatment for those with liver failure or liver cancer, but up to 50% of liver transplant recipients will develop recurrence of PBC (15), and fatigue only resolves in 50% of patients after transplantation (16). Because the pathophysiology of fatigue is still unknown, effective treatments are lacking. Therefore, fatigue, the most common symptom, becomes the most common factor affecting patients' mental health, social well-being, and even disability (17). Chronic fatigue can lead to

depression, anxiety, and cognitive impairment, which induces social isolation and the inability to work and cope with daily life (18). Further research is needed to uncover the mechanisms and develop effective therapies for this challenging symptom.

## **1.2 PBC and autoimmunity**

PBC is considered to be an autoimmune disease because over 90% of patients have autoantibody AMA (14). AMA are reactive to the E2 components of 2-oxoacid dehydrogenase family (2-OADC) including pyruvate dehydrogenase complex (PDC), 2-oxoglutarate dehydrogenase complex (OGDHC), and branched chain 2-oxoacid dehydrogenase complex (BCKDH) (19-21). All three enzymes are encoded within the nucleus and are imported to the mitochondrial inner membrane, where they play key roles in energy homeostasis. Pyruvate is converted to acetyl coenzyme A by the PDC (22). The OGDHC catalyzes the overall conversion of 2-oxoglutarate (the same as alpha-ketoglutarate) to succinyl-CoA and CO<sub>2</sub> (23), while the BCKDH is involved in the breakdown of the branched-chain amino acids isoleucine, leucine, and valine (24). In addition, other antinuclear antibodies (ANA) such as anti-gp210 and anti-sp100 are expressed in PBC patients, especially in AMA-negative sera (25, 26). ANA are serological markers found in a variety of autoimmune diseases including rheumatoid arthritis, systemic lupus erythematosus, autoimmune hepatitis, and inflammatory bowel disease (27-30).

Autoantibody-production B lymphocytes are found at a high frequency of 0.16% in patients peripheral blood with PBC, compared to less than 0.01% in individuals with chronic hepatitis C virus infection and in healthy subjects. The number of autoreactive CD4 T cells and CD8 T cells is significantly higher in the liver than in the blood of patients with PBC. For example, CD4+

helper T cells specific to the PDC-E2<sub>163-176</sub> epitope in PBC patients' peripheral blood are estimated to be  $3.66 \times 10^{-7}$ , while those in the liver with a frequency of  $1.66 \times 10^{-5}$  to  $4.13 \times 10^{-5}$  (31, 32). The frequency of PDC-E2<sub>159-167</sub> specific CD8 T cells was  $4.14 \pm 0.95 \times 10^{-4}$  in the liver and  $3.58 \pm 3.26 \times 10^{-5}$  in the peripheral blood, while in most autoimmune diseases, the frequency of autoantigen-specific CD4+ and CD8+ T cells in the blood is typically around 0.01% to 1% of the total T cell population (33).

Thus, the level of AMA or ANA cannot predict the disease's prognosis, and some AMA positive individuals do not develop liver disease at all (34). Unlike other autoimmune disease, immunosuppression is not standard of care for the management of PBC (3). B cell depletion therapy, particularly with rituximab (an anti-CD20 monoclonal antibody), has shown potential activity in reducing AMA levels, but limited efficacy in improving biochemical markers and alleviating clinical symptoms such as fatigue (35). Liver transplant (LT) recipients with PBC are more likely to develop earlier and more severe recurrent disease with the use of more potent immunosuppression regimens (15). Taken together, these observations cast a degree of doubt concerning an autoimmune etiology and pathogenesis of PBC, even though AMA have proven to be a specific diagnostic marker for disease.

### **1.3 Environmental disease triggers**

Although the pathogenesis and generation of autoimmune responses in PBC is still unclear, the common opinion is that some environmental factors may breakdown the immune tolerance to mitochondrial antigens. Several lines of research have identified viral infection, bacteria, certain toxins and chemicals as environmental factors and triggers of PBC (3).

Several studies have indicated a significant association of a history or recurrence of urinary tract infection (UTI) with PBC (36). *Escherichia coli* (*E. coli*), a predominant urinary tract pathogen, was shown to share a significant immunodominant epitopes of human PDC-E2 (37). The theory that *E. coli* infection leads to the breakdown of tolerance against PDC-E2, was not backed up by further experiment to explain why the autoimmune reactivity mediated by *E. coli* infection only induced liver injury; nor have any animal models been developed to illustrate this possibility in PBC.

The Human betaretrovirus (HBRV) is another PBC trigger that was previously identified by our lab. First, the nucleic acid sequences of HBRV with 93% to 97% similarities of Mouse mammary tumor virus (MMTV) genome sequence were cloned from perihepatic lymph nodes and biliary epithelial cells of patients with PBC (38). Then, RT-PCR was used to detect HBRV RNA in 73% of PBC patients' lymph nodes and 29% of PBC patients liver samples (39). The viral capsid protein was characterized in the lymph nodes of PBC by immunofluorescence with anti-MMTV p27, which was not found in liver disease control lymph nodes (39).

#### **1.4 Genetic factors**

Genetic predisposition is thought to play a significant role in PBC because of a high concordance rate (0.63) in monozygotic twins as compared to dizygotic twins (40). Further, the relative risk for first-, second-, and third-degree relatives of PBC patients was observed to be 9.13, 3.16, and 2.59, respectively (41). Subsequently, genome-wide association studies (GWAS) have provided an important contribution to our understanding the genetics of PBC. The GWAS data from Europe, Japan, North America and China provided many different genetic susceptibility loci.

In particular, the highly polymorphic human leukocyte antigen (HLA) region that encodes loci from the major histocompatibility complex (MHC) and other immune response genes have been mapped (42). Over 50 genome-wide significant associated HLA variants have been identified; DRB1\*08, DRB1\*04, DQA1\*04, DQB1\*04, and DPB1\*03 that are considered causative alleles, whereas DRB1\*11, DRB1\*13, DQB1\*06, DQB1\*03, DQBQ\*15 and DPB1\*04 are protective ones (42-45). Additionally, many non-HLA genes alleles have been linked with PBC, including, MMEL1, IL12RB2, STAT4, CD28, CD58, DENND1B, STAT4, PLCL2, TIMMDC1, IL12A, NFKB1, IL7R, IL12B, HLA, LINC03004, ELMO1, TNPO3, CCDC88B, CXCR5, TNFRSF1A, ATXN2, TNFSF11, DLEU1, RAD51B, EXOC3L4, CLEC16A, IL21R, IRF8, IKZF3, HROB, TYK2, SPIB, SYNGR1, ORMDL3, CD80, IL21, ARID3A and IL16 (46-48). Only a limited number of these genes have been identified as functionally related to the pathogenesis of PBC. Notably, gene variants in the IL12 signaling pathway (IL12A, IL12RB2, STAT4, TYK2, and IL12B) have shown a strong association with PBC (49). IL-12 is involved in the differentiation and activation of T cells and Natural Killer (NK) cells. It drives the switch toward Th1 responses to produce interferon-gamma (IFN- $\gamma$ ) (49, 50). A recent study has revealed enhanced sensitivity of Treg cells from PBC patients to low doses of IL-12 promoting their differentiation into IFN- $\gamma$  secreting cells (51).

### **1.5 Interplay between cholangiocytes and immune cells**

In the early stages of PBC, the portal-based inflammation and florid bile duct lesions mainly restricted to the intrahepatic bile ducts can be observed in liver biopsy tissues. The small interlobular bile ducts within the portal tracts are surrounded by an intense inflammatory infiltrate

composed primarily of CD4+ and CD8+ T cells, B lymphocytes, plasma cells, macrophages, NK and NKT cells, and some eosinophils (52). The cholangiocytes can be observed undergoing immune mediated cell death and occasional granulomatous formation is observed. Progressive biliary damage eventually results in ductopenia and fibrosis (53). Therefore, the interaction between biliary epithelial cells and inflammatory cells is a very important mechanism to understand.

It has been suggested that cholangiocytes are the target of an autoimmune response recognized by autoreactive T cells and AMA focusing on the PDC-E2 like molecule aberrantly expressed on the surface of the biliary epithelial cells in PBC (54). In addition, most of the small cholangiocytes in PBC express major histocompatibility complex (MHC) class I and II molecules, which allow them to act as antigen-presenting cells (55). Therefore, some have hypothesized that a microbial molecular mimic of PDC-E2 or alternatively, AE2 deficiency may induce overexpression of PDC-E2 like molecules on cholangiocytes that in turn leads to the autoimmune response (56).

However, another hypothesis is that a betaretrovirus infection may trigger PBC pathogenesis. Our team found that homogenized lymph nodes from PBC induced the aberrant expression of mitochondrial autoantigen on normal biliary epithelial cells, suggesting that a pathogen in the lymph nodes can trigger this mitochondrial phenotype. Our lab's subsequently characterized a human betaretrovirus infection in the lymph nodes of PBC and colocalized the viral capsid protein to the aberrant autoantigen expression in the same cells (Figure 1) (39). We also found that normal BEC developed the aberrant expression of the PDC-E2 like autoantigen and cytoplasmic localization of the betaretrovirus capsid protein after it was cocultured with PBC lymph node homogenates (Figure 2) (39). Others found that the overexpression of the PDC-E2 like molecule on biliary epithelial cells surface in the allograft of PBC after liver transplantation, suggesting

recurrent disease could be triggered by a residual infection (57). Therefore, we are working on the hypothesis that chronic betaretroviral infection may exist in BECs and lymphocytes, which triggers the aberrant autoantigen expression and a range of immune responses.

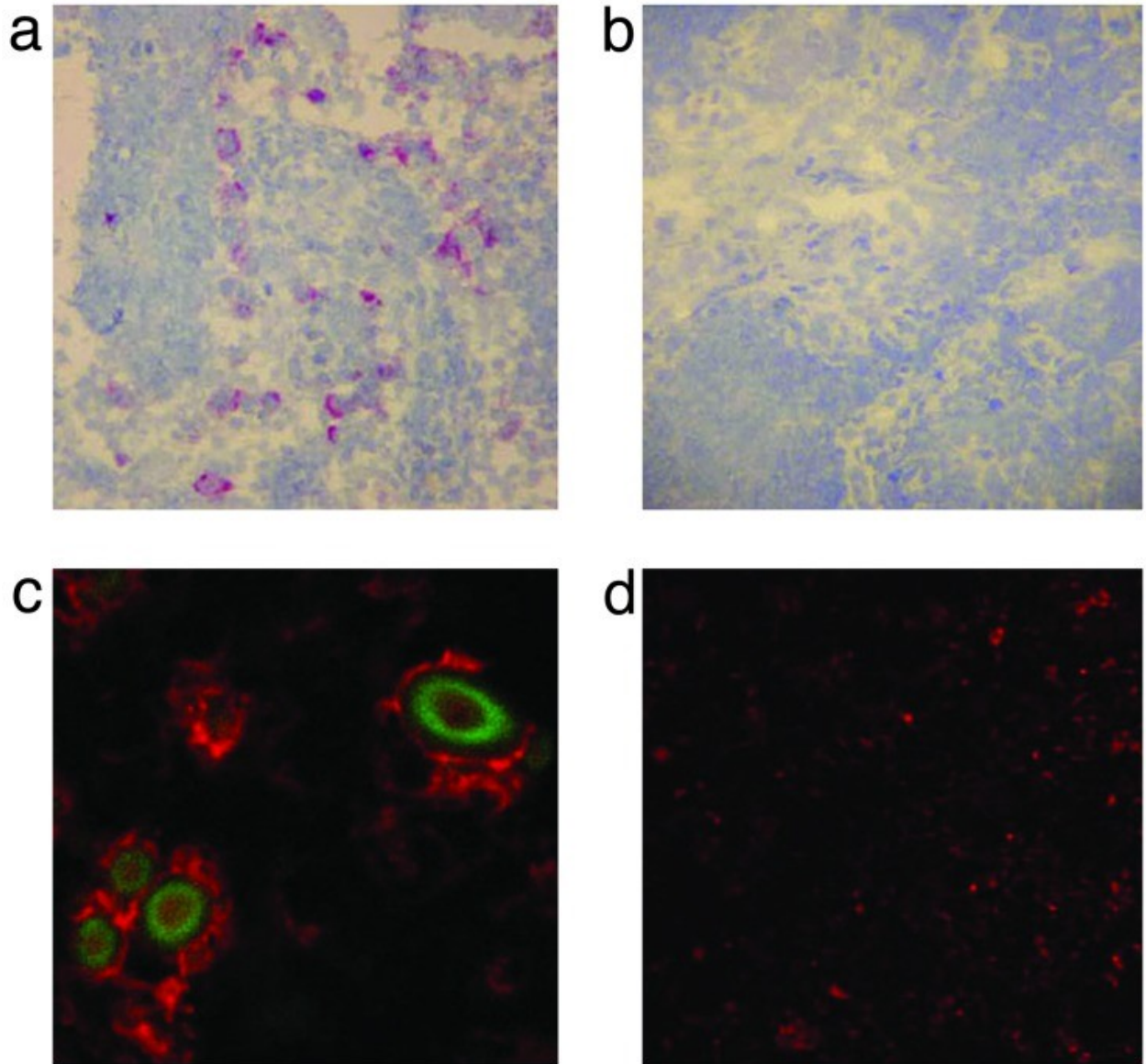


**Figure 1. Immunohistochemistry studies show viral capsid protein in PBC patient's periportal lymph nodes in the same distribution as aberrant autoantigen expression**

(a) PBC lymph node displays a peri-sinusoidal distribution of anti-p27CA reactivity where macrophage/monocyte cells are located. (b) Anti-p27CA reactivity is absent from a control lymph

node from a patient with primary sclerosing cholangitis (PSC). (c and d) Aberrant expression of PDC-E2 in the PBC lymph node but not in the PSC lymph node control. Plasma membrane localization of mitochondrial antigen can be seen by fast red stain of AMA in (c), but only mitochondrial staining can be seen in (d). Cellular colocalization of FITC-stained (green) anti-p27CA in the cytoplasm is observed with aberrant AMA staining in (c). (Original magnification:  $\times 100$  for a and b and  $\times 400$  for c and d.)

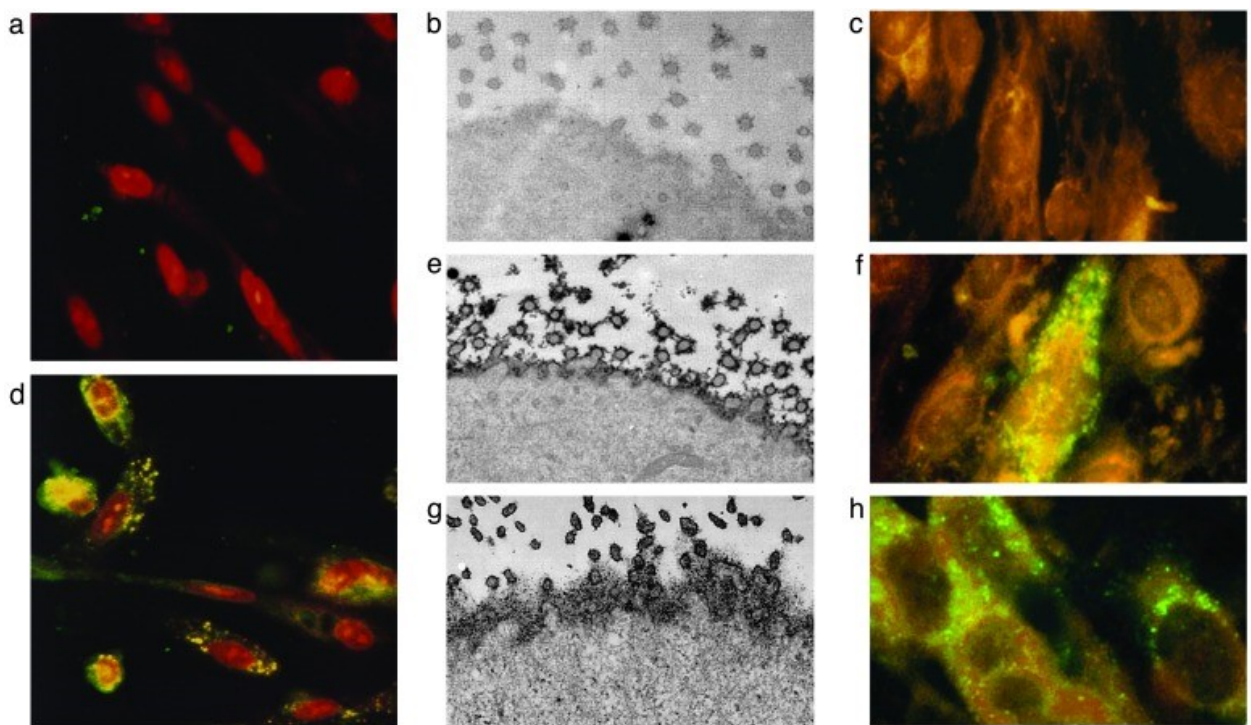


**Figure 2. Normal BEC develop the phenotypic manifestation of PBC when incubated with PBC patient's lymph node homogenates**

(a–c) Before coculture, studies in normal BEC show no AMA staining by immunofluorescence (a), no cell surface expression of PDC-E2 by immunoelectron microscopy (b), and no evidence of viral proteins by immunofluorescence (c). (d–g) After coculture with PBC patient's lymph node homogenates, the BEC develop aberrant PDC-E2 expression after 7 days in culture (d), with cell

surface AMA reactivity on BEC (e) that is similar to that seen in PBC BEC (g), and evidence of cytoplasmic localization of betaretrovirus capsid protein (f). (h) Normal BEC incubated with supernatant from MMTV-producing MM5MT cells also show a similar punctate, cytoplasmic signal from the anti-p27CA immunofluorescence.

## **1.6 Metabolic dysregulation and mitochondrial dysfunction in PBC cholangiocytes**

Our lab's previous proteomic studies showed that primary BEC isolated from PBC liver had upregulated proteins in glycolysis pathway and HIF1 signaling pathway compared to control BEC by STRING functional enrichment (Figure 3) (94). Furthermore, elevated levels of intracellular and extracellular lactate were observed in cultured BEC of PBC by <sup>13</sup>C glucose tracer studies (Figure 4) (94). In addition, we observed decreased glutamine levels in PBC versus control BEC, which is consistent with glutaminolysis in PBC cholangiocytes (Figure 5). This pathway is activated when pyruvate is preferentially converted to lactate by glycolysis and as a result, reduced substrates are available for the TCA cycle. Seahorse studies supported these observations by revealing an increased extracellular acidification rate (ECAR) in PBC BEC although the oxygen consumption was comparable in PBC BEC and control BEC (Figure 6) (94). The accumulated data suggests the presence of aerobic glycolysis in PBC cholangiocytes. As mitochondria perform a critical function related to energy production, metabolism and cellular homeostasis, the metabolic dysregulation may demonstrate mitochondrial dysfunction. The increased mitochondrial DNA copy number in PBC BEC also provided an indication of mitochondrial biogenesis which may compensate for mitochondrial dysfunction (Figure 7) (94).

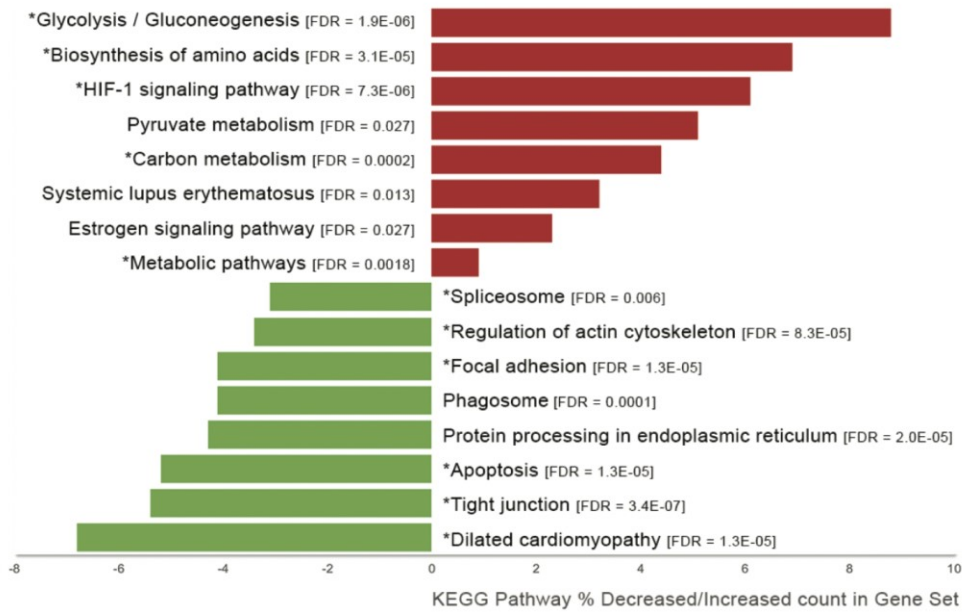


**Figure 3. Normal BEC develops the phenotypic manifestation of PBC when incubated with PBC patient's lymph node homogenates**

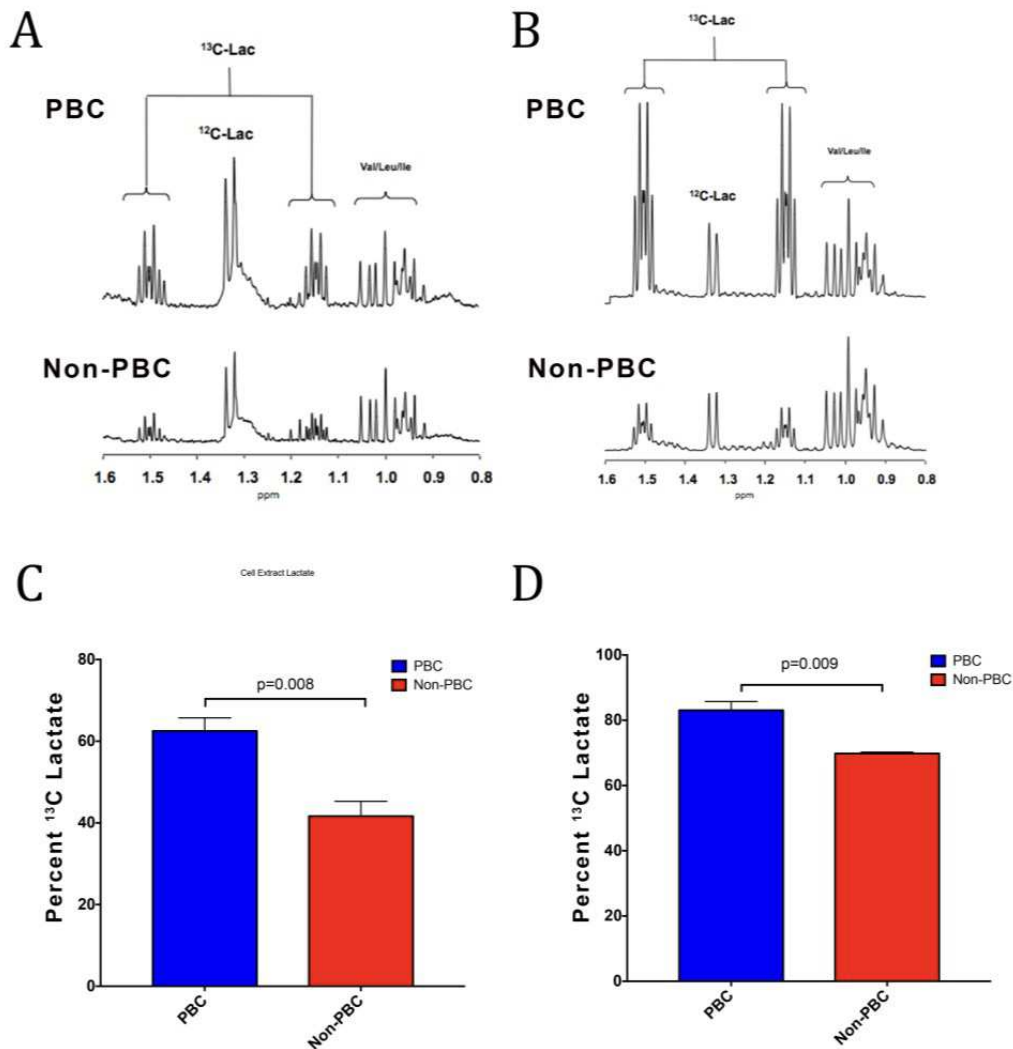


**Figure 4. Cultured biliary epithelial cells (BEC) from patients with Primary Biliary Cholangitis (PBC) show elevated levels of intracellular and excreted lactate in  $^{13}\text{C}$  glucose tracer studies**

Representative sections of  $^1\text{H}$  NMR spectra of cell extracts (A) and lyophilized incubation media (B) after a 24-h incubation with DMEM containing 25 mM  $[\text{U-}^{13}\text{C}]$  show elevated levels of intra- and extracellular lactate, respectively, in PBC BEC compared to end-stage liver disease controls. Significantly higher enrichment of intracellular (C) and extracellular (D) U- $^{13}\text{C}$  in lactate in PBC

BEC (cell lysates n=4; cell supernatant n=3) compared to end-stage liver disease controls (cell lysates and cell supernatant n=3).

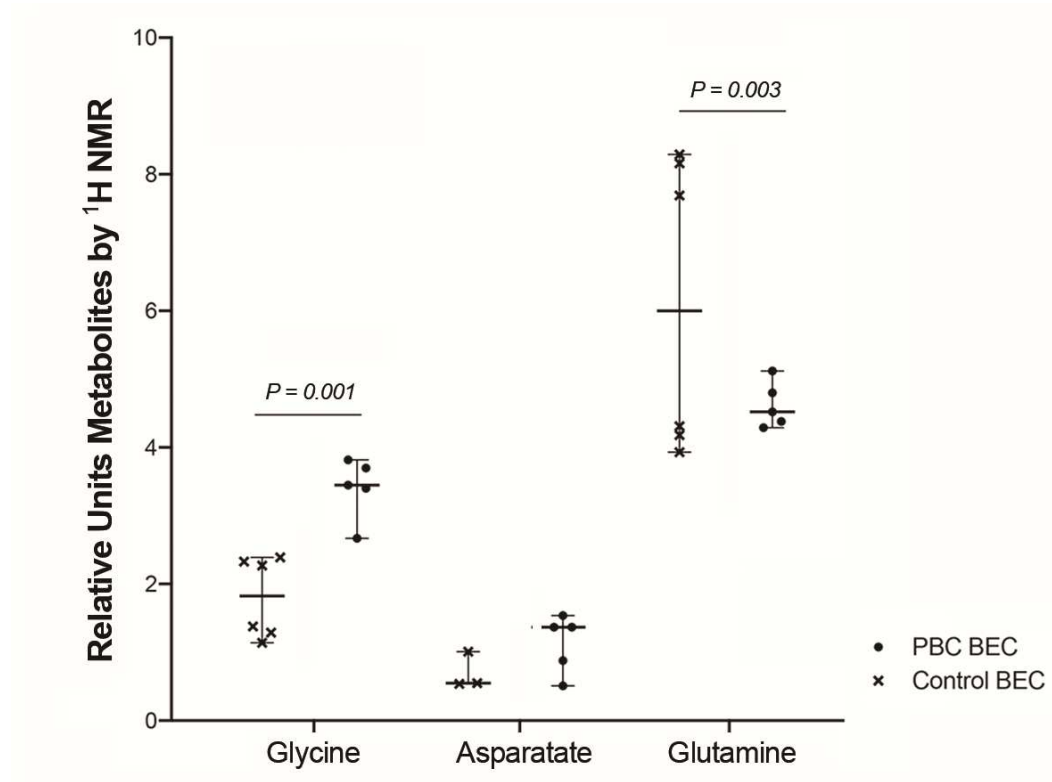


**Figure 5. Intracellular levels of amino acids detected by 1H NMR of cultured biliary epithelial cells (BEC) from patients with Primary Biliary Cholangitis (PBC)**

Representative sections of 1H NMR spectra of cell extracts after a 24-h incubation with DMEM containing 25 mM [U-13C] show elevated levels of glycine and decreased levels of glutamine in PBC cholangiocytes compatible with glutaminolysis as an alternative source for the TCA cycle in PBC BEC (n=5) compared to end-stage liver disease controls (n=6). Data shown as median and IQR (Two-tailed Mann-Whitney test).

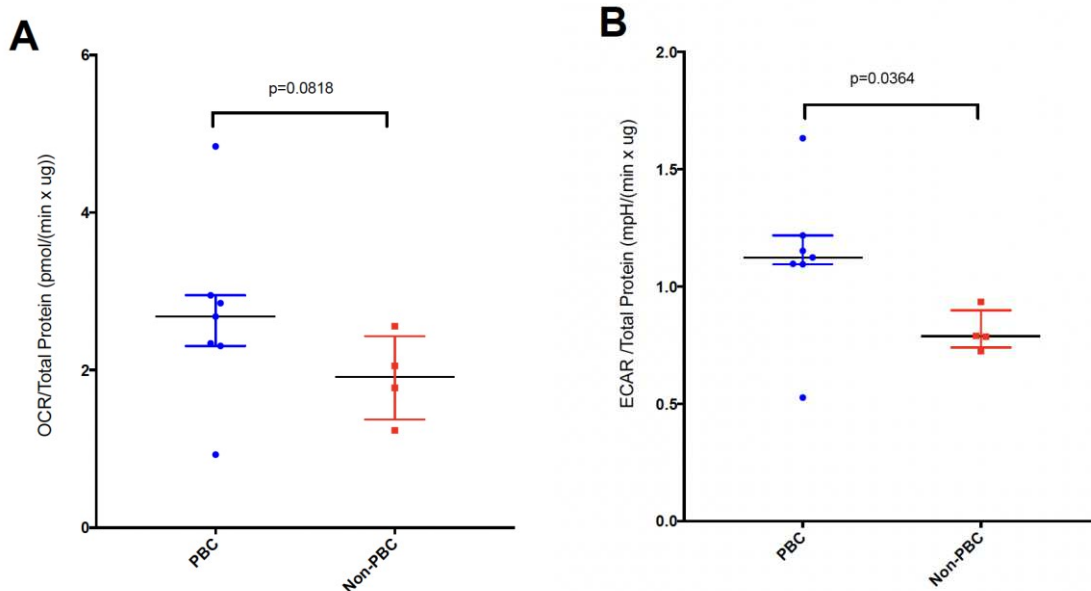


**Figure 6. Significantly increased levels of extracellular acidification rate (ECAR) and trend for elevated oxygen consumption rate (OCR) in Primary Biliary Cholangitis (PBC) patients' biliary epithelial cells (BEC)**

Similar levels of oxygen consumption rate (OCR; A) were observed between cultured PBC BEC (n=7) and end-stage liver control BEC (n=4), while elevated extracellular acidification rate (ECAR; B) was observed in PBC BEC, as measured by the Seahorse XF24 platform.

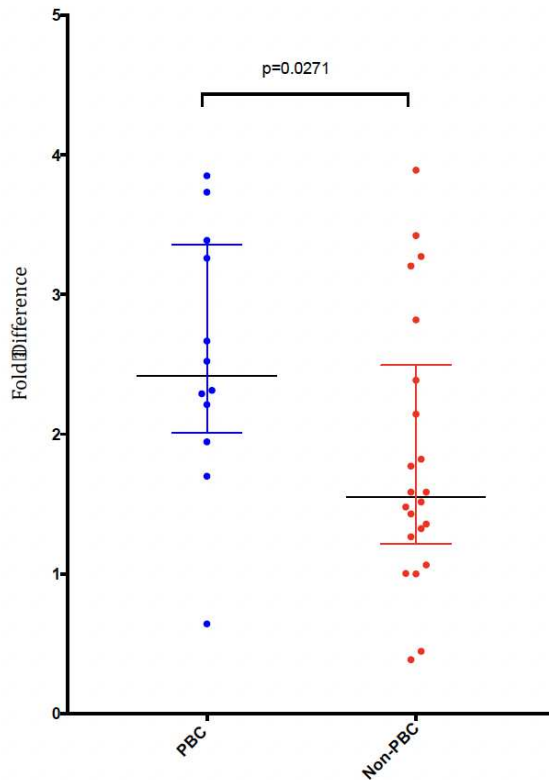


**Figure 7. Significantly higher levels of mitochondrial DNA (Mt-DNA) copy number in Primary Biliary Cholangitis (PBC) patients' biliary epithelial cells (BEC)**

Cultured PBC BEC (n=12) extracted from explanted livers show significantly higher levels of Mt-DNA compared to liver disease controls (n=22) as assessed by quantitative PCR (qPCR).

### 1.7 Hypoxia-inducible factor 1 $\alpha$ (HIF1 $\alpha$ )

Hypoxia-inducible factor 1 $\alpha$  (HIF1 $\alpha$ ) was initially characterized as a critical transcription factor for hypoxia adaptation (58, 59). Under normoxic conditions, HIF1 $\alpha$  is rapidly degraded by the proteasome regulated by the oxygen-dependent prolyl hydroxylase domain protein (PHD)-von Hippel-Lindau tumor suppressor protein (VHL) axis. Under hypoxic conditions, PHD activity is

reduced leading to stable HIF- $\alpha$  subunit expression. HIF1 $\alpha$  is translocated to the nucleus, where it dimerizes with HIF-1 $\beta$  and activates the transcription of various genes involved in adaptive responses to low oxygen (60, 61). Recent studies have described an oxygen-independent HIF1 $\alpha$  signaling phenotype referred to as ‘pseudohypoxia’, which is associated with succinate accumulation induced by dysfunctional succinate dehydrogenase (SDH) subunits, OGDHC and lipoic acid synthase (LIAS) (62-65). It is notable that a variety of pathways are regulated by HIF1 $\alpha$  signaling activation that include cell proliferation, apoptosis, angiogenesis, glucose metabolism, immune cell activation, and survival (66).

## **1.8 Hypothesis**

The aberrant overexpression of mitochondrial autoantigens on BEC and the abundance of sera AMA are the distinguishing features of PBC, but the mechanism by which these mitochondrial phenotypes are generated is still unclear. We found a mitochondrial dysfunction mediated metabolic remodeling observed in PBC BEC, and the accumulation of mitochondrial autoantigens may occur as a result of compensatory mitochondrial biogenesis. Moreover, a human betaretrovirus infection has been characterized in PBC patients’ lymph nodes and cholangiocytes and, mitochondrial autoantigens are located in the same cells within lymph nodes. Co-cultivation studies show that lymph nodes homogenates from PBC can induce the aberrant overexpression of mitochondrial autoantigens and viral proteins in healthy BEC. Therefore, we hypothesize that the overexpression of mitochondrial autoantigens and the metabolic remodeling will be found in PBC bile ducts and in peripheral blood. This is based on the assumption that viral infection triggers the mitochondrial phenotype in PBC cholangiocytes and lymphocytes. Therefore, we chose to study

the metabolic changes and the expression of mitochondrial autoantigen in cholangiocytes and PBMC from patients with PBC.

### **1.9 Implications and importance of investigation**

The etiology and pathogenesis of PBC are poorly understood, and UDCA is the only first line therapy, but up to 46% of patients fail to respond to it. Most of these patients experience liver failure in the end (67). Moreover, there is no treatment to relieve fatigue which impacts patients' mental health and social well-being. Thus, further research on the systemic metabolic remodeling, mitochondria function and the mechanism of aberrant overexpression of mitochondrial autoantigen will provide deeper understanding of the disease pathogenesis.

## **Chapter 2: Materials and Methods**

### **2.1 Detections of Enolase 1 and PDC-E2 in liver tissue by immunohistochemistry**

Paraffin-embedded liver tissue from PBC patients (n=4) and control subjects (n=3) was cut onto glass slides at a 4 µm thickness, deparaffinized and then hydrated. Antigen retrieval was performed using Tris buffer (PH 10.0) at 95°C for 20 min for ENO1 and PDC-E2. Tissue sections were blocked with protein blocking solution or goat serum for 45 min at room temperature. The primary antibody, Rabbit monoclonal anti-ENO1 (abcam, ab 155955, 1:50), was incubated overnight at 4°C. AMA affinity purified from PBC patient serum using the AminoLink Plus Immobilization kit (Pierce, Rockford, IL) were used as the primary antibody at a concentration of 25 µg/ml overnight at 4°C. Following rinsing, endogenous peroxidase activity was quenched using 3% H<sub>2</sub>O<sub>2</sub> for 10 min. Tissue sections were incubated with HRP-anti-Rabbit Polymer or Goat anti-Human IgG H&L (HRP) (abcam, ab 6858, 1:1000) for 45 min, and developed with 3,3'-diaminobenzidine (DAB) (Dako, K3467). The protein blocking solution and HRP-anti-Rabbit Polymer were from the Ready-to-use IHC kit (BioVision, K405).

The images were analyzed using ImageJ. The average optical density (AOD) was calculated after measuring the integrated optical density (IOD) and area on ten randomly selected bile ducts and nearby hepatocytes (5-10 cells) in each tissue section using the formula:  $AOD = IOD/area$ .

### **2.2 Detections of HIF1α, PDC-E2 and CK19 in liver tissues by immunofluorescence**

Paraffin embedded liver tissue from PBC patients (n=4) and control subjects (n=3) were cut onto glass slides at a 4  $\mu$ m thickness, deparaffinized and then hydrated. Antigen retrieval was performed using Tris-EDTA buffer (PH 9.0) at 95°C for 20 min for HIF1 $\alpha$ , PDC-E2, and CK19. Tissue sections were incubated with 0.25% Triton buffer for 15 minutes which was subsequently replaced with Image-iT™ FX Signal Enhancer (Thermo Fisher Scientific, I36933) for 30 minutes. Following rinsing, the tissue sections were blocked with 10% donkey serum for 1 hour at room temperature. This was then replaced by a primary antibodies mix solution including Rabbit monoclonal anti-HIF1 $\alpha$ , (Abcam, ab51608, 1:50), AMA (Lab made, 25  $\mu$ g/ml), and mouse monoclonal anti-CK19 (Abcam, ab7755, 1:100). The sections were incubated overnight at 4°C. Following rinsing, the tissue sections were incubated with a secondary antibodies mix including Donkey anti-Rabbit IgG Alexa Fluor™ 647 (Invitrogen, A-31573, 1:1000), Donkey anti-mouse IgG Alexa Fluor™ 555 (Invitrogen, A-31570, 1:1000), and Donkey Anti-Human IgG Alexa Fluor® 488 AffiniPure™ (Jackson ImmunoResearch, 709-545-149, 1:1000) for 1 hour at room temperature. Then DAPI was applied to the sections for 10 minutes of incubation. Following rinsing, the mounting solution and cover slides were added. The photomicrographs were taken by a confocal microscope Zeiss LSM-710.

## **2.3 Visualization analysis of whole blood RNAseq data**

### **2.3.1 Differential gene expression analysis**

Our lab colleagues did the Next-generation sequencing on PBC whole blood total RNA samples and healthy control whole blood total RNA samples. The PBC samples (n=88) were baseline samples pretreated by Obeticholic Acid (OCA), and were provided by a clinical trial called the

POISE study (ClinicalTrials.gov, number NCT01473534). The healthy control samples (n=13) were collected from Dr. Andrew Mason's clinic or donated by volunteers. Hussain Syed did the bioinformatic data processing. He combined transcripts level counts to gene level counts, then normalized them by the variance stabilizing transformation (VST) method. Transcripts per Million (TPM) counts were obtained for downstream analysis. The Deseq2 R package was used to do differential expression analysis with negative binomial generalized linear models. The adjusted p-value of genes with significant differential expression was below 0.05.

### **2.3.2 Visualization analysis of genes in glycolysis, TCA cycle, ETC and OXPHOS**

To identify systemic metabolic changes in glycolysis, TCA cycle, ETC and OXPHOS and OXPHOS, Hussain and I investigated all the significant differentially expressed genes involved in these pathways and compared the log<sub>2</sub> fold changes of the TPM of PBC/healthy, and showed those changes by heatmaps.

## **2.4 Mitochondrial DNA quantitative PCR**

### **2.4.1 DNA extraction**

Whole blood DNA samples (n=106) from the POISE study were provided by Intercept Pharmaceuticals and were stored at -80°C. Whole blood DNA samples of healthy controls (n=16) were extracted using a QIAamp Blood Mini kit (Qiagen, Toronto, ON, Can) following the manufacturer's instructions from PAXgene blood RNA tubes collected from several clinics, then stored at -80°C. Before performing the experiments, the DNA concentration and quality were assessed using a Nanodrop 1000 prior to performing experiments.

#### **2.4.2 qPCR for mtDNA copy number**

The relative abundance of mitochondrial DNA (mtDNA) was assessed using real-time quantitative polymerase chain reaction (qPCR). A pre-designed FAM-MGB TaqMan assay was used to assess the copy number of the mitochondrial D-loop region (Hs02594861\_s1, ThermoFisher Scientific, Waltham, MA, USA). The TagMan assay of beta-2-microglobulin (B2M) (Hs99999907\_m1, ThermoFisher Scientific, Waltham, MA, USA) was assessed as nuclear DNA which was used for normalization. All reactions were run on MicroAmp Optical 384-well reaction plates (ThermoFisher Scientific, Waltham, MA, USA). The D-loop assay was carried out in 10  $\mu$ L reaction volumes consisting of the following: 5 $\mu$ L TaqMan Universal PCR Master Mix (ThermoFisher Scientific, Waltham, MA, USA), 0.5  $\mu$ L TaqMan D-loop Expression Assay, and 4.5  $\mu$ L DNA diluted in commercial Ultrapure RNase/DNase free water (Gibco, Waltham, MA, USA). After the samples were loaded, the plates were covered with MicroAmp Optical Adhesive Film (ThermoFisher Scientific, Waltham, MA, USA) and spun at 300 g for 3 minutes. The reactions were run in the ABI 7900HT Real-Time PCR System, which continuously monitored fluorescence spectra. The cycling condition included an initial phase of 2 min at 50 °C, followed by 10 min at 95 °C, then 40 cycles of 15 s at 95 °C and 1 min at 60 °C. The B2M assay was carried out in 10  $\mu$ L reaction volumes consisting of the following: 5  $\mu$ L TaqMan Universal PCR Master Mix (ThermoFisher Scientific, Waltham, MA, USA), 0.5  $\mu$ L TaqMan B2M Expression Assay, and 4.5  $\mu$ L DNA diluted in commercial Ultrapure RNase/DNase free water (Gibco, Waltham, MA, USA). Each sample was assayed in duplicate, two wells were used as no template background controls with only water added. The cycling condition included an initial phase of 10 min at 95 °C, 40 cycles of 15 s at 95 °C, 15s at 95°C and 1 min at 60 °C. D-loop levels were normalized to B2M

levels using the  $\Delta\text{Ct}$  method. First,  $\text{Avg. Ct}^{\text{D-loop}} - \text{Avg. Ct}^{\text{B2M}} = \Delta\text{Ct}$ , then,  $2^{-\Delta\text{Ct}} = \text{Fold Difference}$ . The fold difference was the mtDNA copy number.

## **2.5 Evaluation of mitochondrial membrane potential in PBMC**

Some cryopreserved PBMC of PBC (n=9), NASH (n=8), and healthy control (n=8) were thawed in 10ml R10 media (RPMI 1640, 10% heat inactivated Fetal Bovine Serum and 1% Penicillin and Streptomycin), and spun at 300g for 10 minutes. They were resuspended in 10ml R10 media and the cells were spun down at 300g for 10 minutes. Then cells were resuspended in 10ml R10 media and were placed in the incubator at 37°C and 5% CO<sub>2</sub>. After 4 hours, the cells were counted and their viability was checked. The cells were spun at 300g for 10 minutes, then resuspend in HBSS to make 5 million/ml single cell suspensions. The MitoProbe™ TMRM Assay (ThermoFisher Scientific, Waltham, MA, USA) was used to evaluate the mitochondrial membrane potential by flow cytometric analysis. Carbonyl cyanide 3-chlorophenylhydrazone (CCCP) was used as a positive control for the induction of mitochondrial membrane depolarization. The PBMC were incubated for 15 minutes with BD Horizon™ Fixable Viability Stain 450 (Cat. No. 562247) at room temperature, then the positive control cells were incubated for 5 minutes with CCCP in an incubator at 37°C and 5% CO<sub>2</sub>. All the PBMC incubated for 30 minutes with TMRM (20nM) in an incubator at 37°C and 5% CO<sub>2</sub> and were then analyzed using a flow cytometer (Fortessa-SORP, SONY). The data for the median of fluorescence intensity (MFI) of the TMRM stain were analyzed by Flowjo.

## **2.6 Evaluation of AMA reactivity in PBMC by immunocytochemistry**

Some cryopreserved PBMC of PBC (n=3), NASH (n=3), and healthy control (n=3) were thawed. Cells were seeded on glass slides and were fixed by flow fixation buffer in room temperature for 20 minutes, then the cells were permeabilized by 0.25% Triton buffer for 10 minutes. After blocking cells by 10% donkey serum and washing them, the slides were incubated with AMA (Lab made, 25 µg/ml) at 4 °C overnight followed by washing and incubation of Donkey Anti-Human IgG Alexa Fluor® 488 AffiniPure™ (Jackson ImmunoResearch, 709-545-149, 1:1000) for 1 hour at room temperature. We washed slides by PBST 3 times, then DAPI was applied to the sections for 10 minutes of incubation. Following rinsing, the mounting solution and cover glass were added. The photomicrographs were taken by a confocal microscope Zeiss LSM-710. The images were analyzed using ZEN software. The MFI of AMA was calculated after measuring the fluorescence intensity of AMA in 8-10 random cells per sample.

## **2.7 Fluorescence-activated cell sorting**

We sorted high-TMRM PBMC and low-TMRM PBMC by Cell sorter Sony MA900 after staining by MitoProbe™ TMRM stain. The gating strategy identified the top 5-8% cells with highest TMRM fluorescence as high-TMRM PBMC and identified the bottom 5-8% cells with lowest TMRM fluorescence as low-TMRM PBMC. Then the cells were seeded on glass slides and were fixed by flow fixation buffer. We stained cells with AMA and DAPI as same as the method mentioned in 2.6. The photomicrographs were taken by a confocal microscope Zeiss LSM-710. The

images were analyzed using ZEN software. The MFI of AMA was calculated after measuring the fluorescence intensity of AMA in 8-10 random cells per image.

## **2.8 Statistical analysis**

Statistical analysis were performed using Prism software (release 9.0). We performed an unpaired Mann-Whitney test for any two groups comparisons and linear regression for ALP and Mt-DNA copy numbers. All levels of  $p < 0.05$  were considered to be significant.

## Chapter 3: Results

### Section 1: Study of metabolic remodeling in PBC cholangiocytes

#### 3.1 Increased glycolytic enzyme expression in PBC cholangiocytes

Our previous analysis suggested that cultured primary cholangiocytes had elevated glycolysis because the levels of intracellular and extracellular lactate were increased in PBC BEC vs. non-PBC BEC. Furthermore, the glycolysis pathway was upregulated in PBC BEC vs. non-PBC BEC by STRING enrichment analysis of proteomics, including aldolase (ALDOA), glyceraldehyde 3-phosphate dehydrogenase (GAPDH), enolase (ENO1, ENO2), pyruvate kinase (PKM) and lactate dehydrogenase (LDHA). Because the primary cholangiocytes were derived from patients with end-stage liver disease and cultured in vitro, the cell metabolism may have been impacted by the cell culture. Therefore, we studied liver tissues from patients using IHC for differences in glycolytic enzyme expression. As we confirmed that the small intrahepatic bile ducts had increased AMA reactivity in cholangiocytes compared to hepatocytes, we performed anti-ENO1 reactivity that also demonstrated an increased signal in PBC vs. control with an increased ratio of signal in cholangiocytes vs. hepatocytes (a ratio of 1.87 vs. 0.51 in PBC vs. control,  $P < 0.0001$ ; Figure 8). Therefore, increased glycolytic enzyme expression was observed in cholangiocytes of PBC both in vitro and in vivo, which strengthened the evidence of a metabolic shift characterized by increased aerobic glycolysis in PBC cholangiocytes.

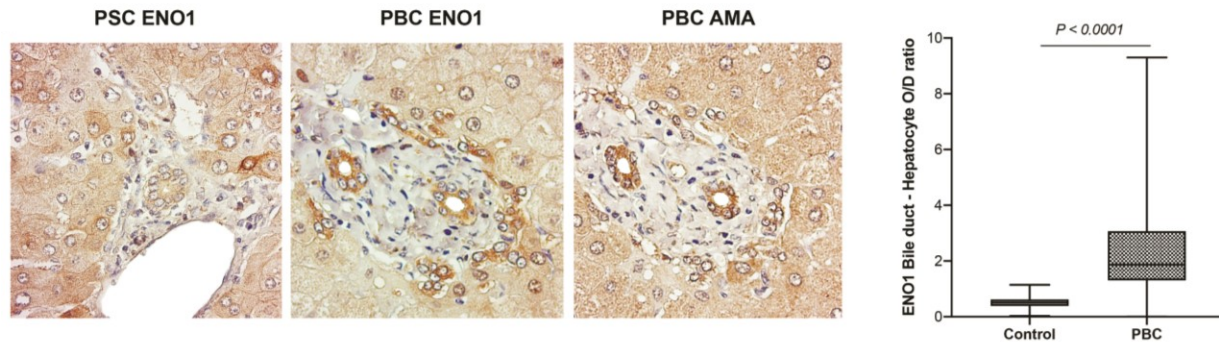


**Figure 8. Increased glycolytic protein expression in PBC cholangiocytes**

Immunohistochemistry with increased anti-ENO1 and AMA reactivity in PBC cholangiocytes (n=4) vs liver disease controls (n=3) [Original magnification x 400]. The box and whisker plot shows the increased ratio of cholangiocytes/hepatocyte optical density (O/D) of ENO1 signal in PBC bile ducts vs. control samples. The box and whisker plot is shown in median, IQR and minimum and maximum range (Two-tailed Mann-Whitney test).

### **3.2 HIF1 $\alpha$ was activated in occasional PBC cholangiocytes**

As an exhibition of a metabolic shift towards aerobic glycolysis was observed in PBC cholangiocytes, we were interested in investigating the mechanism behind this metabolic remodeling. HIF1  $\alpha$  plays a significant role in promoting the use of glycolysis to generate energy in cancer and proliferating cells under both hypoxic and normoxic conditions. Our previous study showed the upregulated HIF1 signaling pathway was highlighted by the STRING enrichment analysis of PBC BEC proteomics (Figure 3). For further investigation, we performed multiplex immunofluorescence to detect HIF1  $\alpha$ , PDC-E2, and Cytokeratin 19 (CK19) in PBC liver tissues vs. controls liver tissues. CK19 is an intermediate filament protein expressed in the epithelial cells,

so we used CK19 as a cholangiocytes marker. Therefore, when all of the small intrahepatic/sublobular cholangiocytes were labeled by CK19, the AMA-PDCE2 reactivity was observed in most PBC cholangiocytes and was not shown in the control cholangiocytes. Then some occasional PBC cholangiocytes exhibited HIF1  $\alpha$  signal in their nuclei (white arrows), which meant that HIF1  $\alpha$  signal was activated in those specific cells. These cells' morphology and the shapes of their nuclei differed from the other cholangiocytes. The chromatin distribution was denser in these cells' nuclei. In contrast, we didn't see any HIF1  $\alpha$  signal in the cholangiocytes of cryptogenic liver disease (crypto) and Non-Alcoholic Steatohepatitis (NASH). (Figure 9)

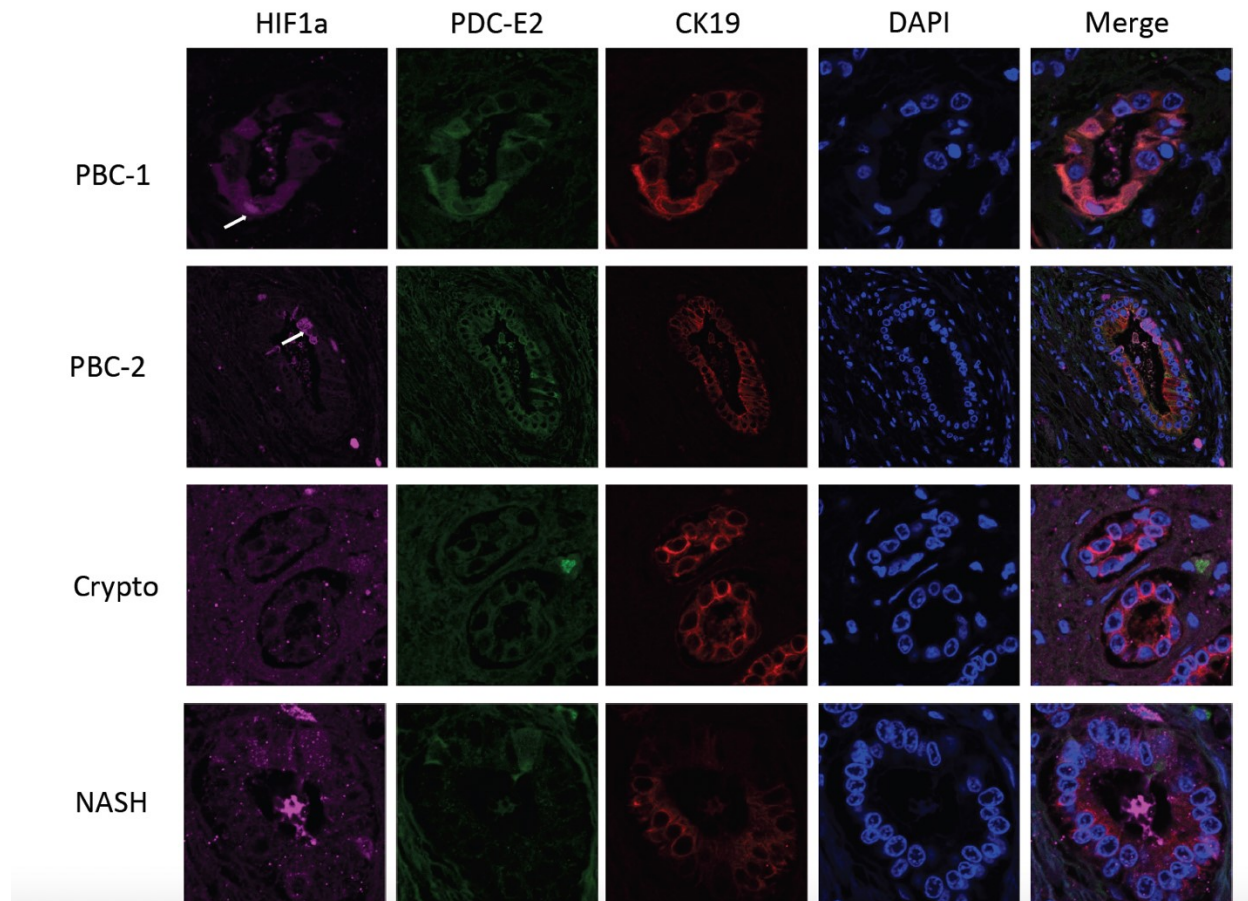


**Figure 9. Activated HIF1 $\alpha$  signaling shown in occasional cholangiocytes in PBC**

Representative photomicrographs of PBC, cryptogenic liver disease (Crypto), and non-alcoholic steatohepatitis (NASH) liver tissue sections stained by multiplex immunofluorescence (IF) with antibodies against HIF1  $\alpha$  (magenta), PDC-E2 (green) and CK19 (red). Nuclei were stained by DAPI (blue). The HIF1  $\alpha$  activated cholangiocytes are indicated by white arrows. The photomicrographs were taken by a Zeiss LSM-710 confocal microscope. Original magnification: x 400, zoom x2.

Interestingly, we found that some cells with activated HIF1  $\alpha$  signal in the sublobular bile ducts of PBC had two nuclei (Figure 10). These nuclei had smaller shapes and denser chromatin distributions, which differed from normal cholangiocytes nuclei.

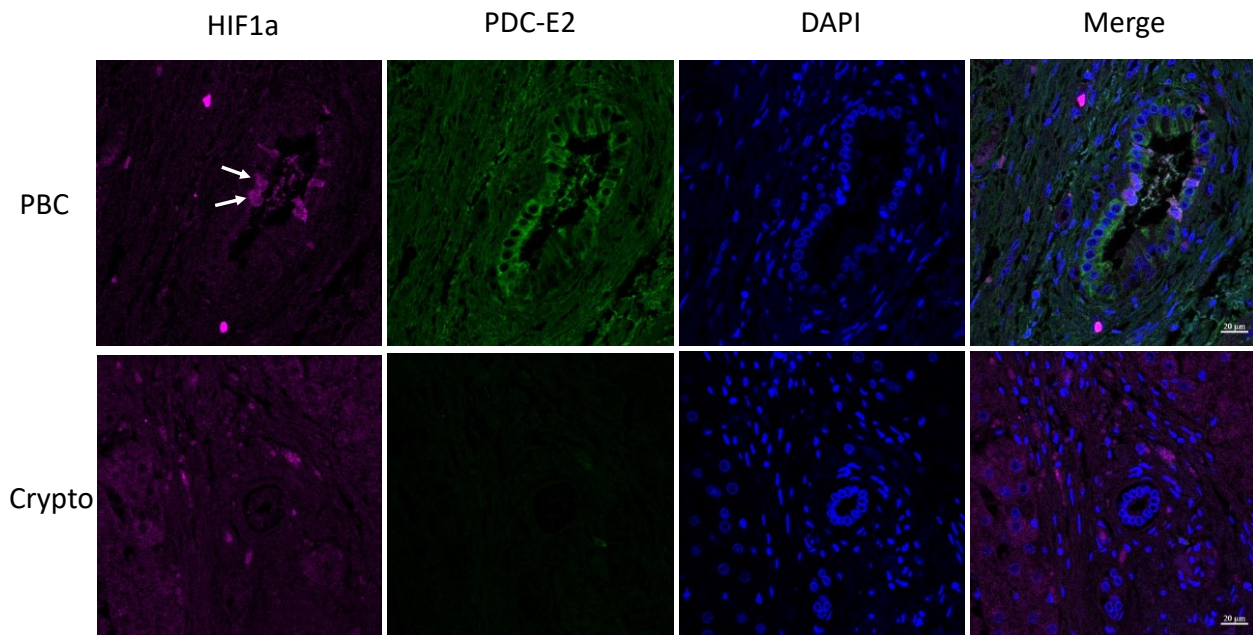


**Figure 10. Double nuclei shown in the cells with activated HIF1 $\alpha$  signaling in PBC**

Representative photomicrographs of liver tissue sections with PBC or Crypto stained by multiplex immunofluorescence (IF) with antibodies against HIF1  $\alpha$  (magenta), PDC-E2 (green), and DAPI (blue). The double nuclei cholangiocytes with activated HIF1  $\alpha$  are indicated by white arrows. The photomicrographs were obtained by a Zeiss LSM-710 confocal microscope. Original magnification: x 400.

## **Section 2: Study of metabolic remodeling in PBC peripheral blood**

### **3.3 Dysregulated transcription of whole blood in glycolysis and the tricarboxylic acid cycle genes in PBC**

To study whether similar metabolic changes occurred in the peripheral blood in PBC, we analyzed glycolysis and the Tricarboxylic Acid (TCA) cycle pathways using differential gene expression analysis data of the whole blood RNAseq in PBC vs. healthy control. As demonstrated in Figure 10, the transcription levels of many glucose metabolism enzymes were significantly upregulated in PBC (labeled with orange), such as Hexokinase (HK1, HK3), Glucose-6-phosphate isomerase (GPI), phosphofructokinase (PFKM, PFKL, PFKP), aldolase (ALDOA, ALDOB, ALDOC), glyceraldehyde 3-phosphate dehydrogenase (GAPDH), enolase (ENO1, ENO2, ENO3), pyruvate kinase (PKM), and lactate dehydrogenase (LDHA, LDHC). Most of these upregulated enzymes catalyze reversible reactions both glycolysis and gluconeogenesis. Interestingly, mitochondrial pyruvate carrier components (MPC1, MPC2) (labeled with green), which are essential for transporting pyruvate from the cytoplasm into the mitochondrial inner membrane, were downregulated in PBC. This illustrated that pyruvate might be blocked from entering the mitochondria. Furthermore, the transcription levels of pyruvate dehydrogenase kinases (PDK2, PDK3, PDK4) were increased in PBC. PDK enzymes can phosphorylate the E1 subunit of the pyruvate dehydrogenase complex, leading to its inactivation, thus inhibiting the conversion of pyruvate to acetyl-CoA. Accordingly, the accumulation of these changes supported a metabolic shift towards aerobic glycolysis in peripheral blood in PBC.

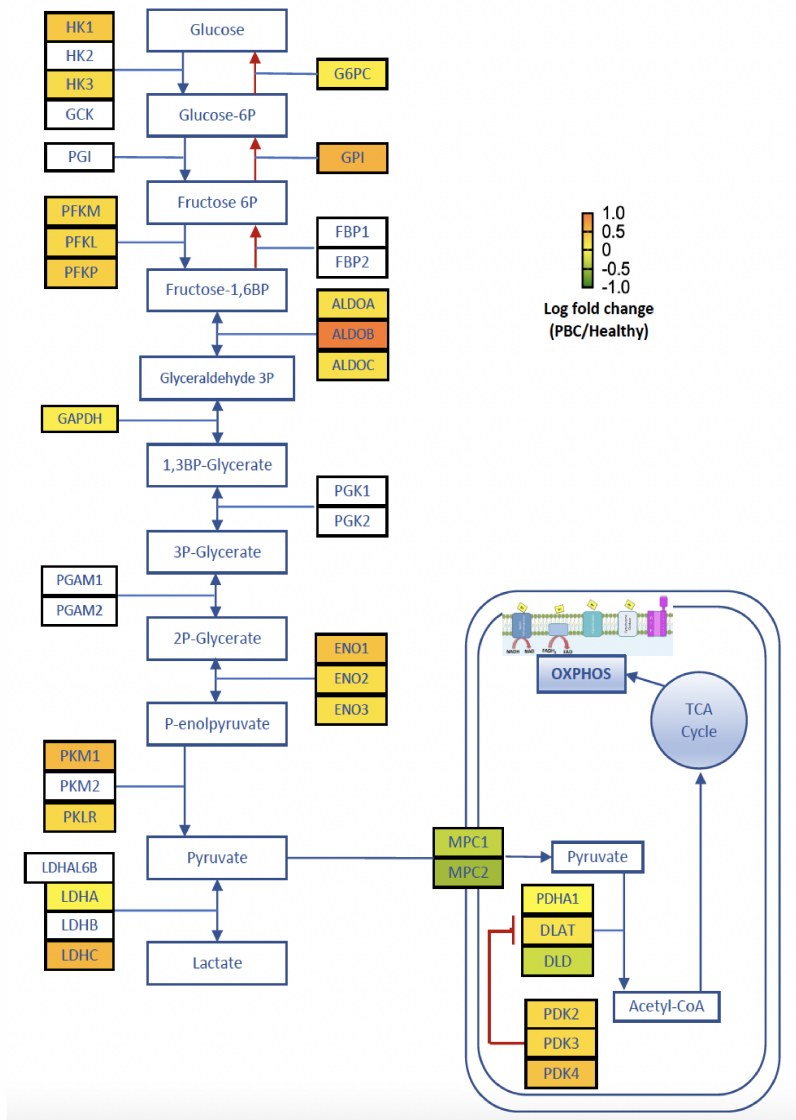


**Figure 11. Pathway map highlighting differentially expressed genes involved in cellular energy metabolism in PBC whole blood RNAseq analysis**

The pathway map was modified from wikipathways map WP534 (Glycolysis/Gluconeogenesis (Homo Sapiens)) by Adobe illustrator. The highlighted genes labelled in orange were significantly upregulated in PBC vs. healthy control, and downregulated genes are labelled in green. The log fold change was log<sub>2</sub> fold changes of TPMs in PBC/healthy control.

### **3.4 Inconsistent transcription levels changes of genes in electron transport chain and oxidative phosphorylation in the whole blood of PBC**

Given the evidence supportive of the peripheral blood of PBC showing a similarly increased aerobic glycolysis phenotype as cholangiocytes, we were interested in how electron transport chain (ETC) and oxidative phosphorylation (OXPHOS), the primary energy production pathways, were altered in the blood of PBC. Both ETC and OXPHOS are located on the mitochondrial inner membrane. ETC transfers electrons from NADH and FADH<sub>2</sub> generated by the TCA cycle to oxygen through four complexes (Complex I-IV), creating a proton gradient across the membrane, in order to synthesize ATP through ATP synthase (Complex V). In total, 91 protein-coding genes are involved in Complexes I – V; 13 of them are encoded by mitochondrial DNA and the others by nuclear DNA. Therefore, the transcription levels of these genes were evaluated using differential gene expression analysis of the data of the whole blood RNAseq in PBC vs. healthy control.

Interestingly, in the volcano plot (Figure 12A), 11 mitochondrial encoded genes (MT-ND1, MT-ND2, MT-ND4, MT-ND4L, MT-ND5, MT-ND6, MT-CYB, MT-CO1, MT-CO2, MT-CO3, MT-ATP6) were upregulated in transcription levels in PBC, and 27 nuclear encoded genes (NDUFA1, NDUFA2, NDUFA4, NDUFA5, NDUFA6, NDUFB1, NDUFB2, NDUFB3, NDUFB6, NDUFS4, NDUFS5, UQCRB, UQCRH, UQCR10, COX6A1, COX6C, COX7A2, COX7A2L, COX7B, COX7C, COX17, ATP5H, ATP5I, ATP5J, ATP5J2, ATP5L, ATP5F1) were downregulated in PBC vs. healthy controls. In the heatmap analysis of transcription expression levels, we generated

a heatmap clustered by both genes (11 mitochondrial-encoded genes and 11 nuclear-encoded genes with the highest Log<sub>2</sub> fold changes) and sample names. Two distinct patterns between the mitochondrial-encoded genes (MT-genes) and nuclear-encoded genes (NC-genes) were shown. One was that MT-genes showed high expression in 53 PBC patients and 1 healthy control when NC-genes were low. The other was that MT-genes showed low expression in 12 healthy controls and 35 PBC patients with highly expressed NC-genes (Figure 12B). The changes suggested that 60% of PBC patients had an upregulation of MT-genes while NC-genes were downregulated. This illustrated inverse changes in transcription levels of components of ETC and OXPHOS, inducing inefficient cellular respiration and energy production in some PBC, which led to an increased reliance on glycolysis.

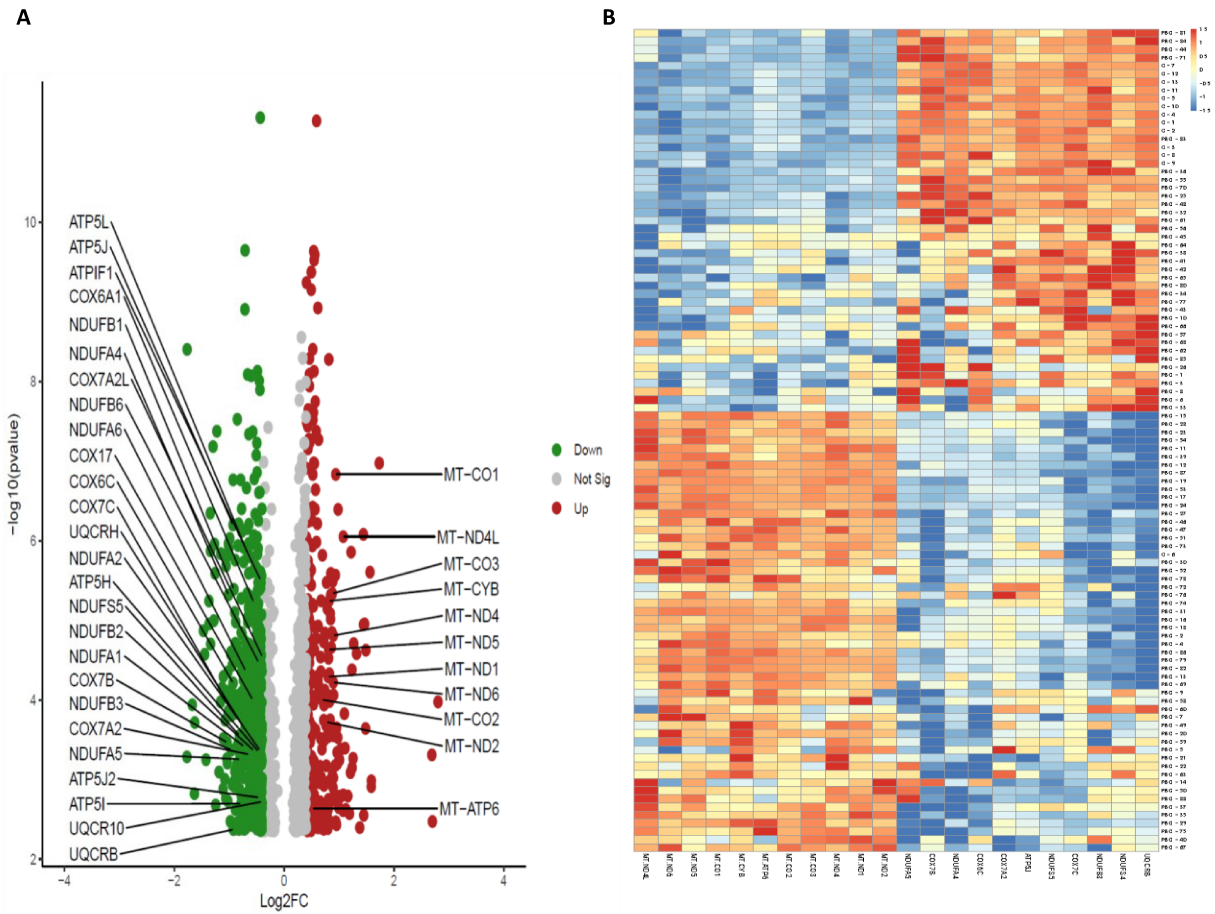


**Figure 12. Abnormal gene expressions of ETC and OXPHOS characterized by upregulated expressions of mitochondrial encoded genes and downregulated nuclear encoded genes in PBC whole blood RNAseq analysis**

(A). Volcano plot showing the differential gene expression between PBC and healthy controls, showing only the points with  $padj < 0.05$ . Upregulated genes in PBC are labelled red and downregulated genes are labelled green. The graph is plotted using ggplot. (B). Heatmap showing the distribution of 11 mitochondrial encoded genes (MT-ND1, MT-ND2, MT-ND4L, MT-ND4, MT-ND5, MT-ND6, MT-CO1, MT-CO2, MT-CO3, MT-CYB, MT-ATP6) and 11 nuclear encoded genes (NDUFA4, NDUFA5, NDUFB3, NDUFS4, NDUFS5, UQCRB, COX6C, COX7A2, COX7B, COX7C, ATP5J) in PBC and healthy controls. The graph was generated by

heatmap with a Hierarchical Clustering feature. TPMs of genes were applied as the intensity of changes. Red represents high expression levels and blue represents low expression levels.

### **3.5 Elevated mitochondrial DNA copy number in PBC peripheral blood**

The mitochondria genome is a small, circular DNA that replicates independently, and both nuclear and mitochondrial transcription factors are able to regulate mitochondrial encoded genes transcription. Because we found that the transcription levels of mitochondrial encoded genes were upregulated in some PBCs, we were curious if mitochondrial DNA replication was increased as well. The mitochondrial DNA (Mt-DNA) replication was quantified by quantitative real time PCR targeting the non-coding D-loop region of Mt-DNA. The Mt-DNA copy number represented the Mt-DNA replication. A gradient increases of Mt-DNA copy number in healthy controls (n=16), responders (n=42), and non-responders (n=60) are shown in Figure 13A. The differences between responders and healthy controls was significant and was even more significant between non-responders and healthy controls,  $p<0.05$  and  $p<0.01$  respectively. However, there was no significant difference between responders and non-responders. All of the samples that had both Mt-DNA copy number and Alkaline Phosphatase (ALP) values were enrolled for the linear regression analysis which illustrated the Mt-DNA copy number was positively correlated with ALP and represents the best prognosis biomarker of PBC (Figure 13B). In conclusion, the Mt-DNA replication was significantly increased in PBC compared to healthy controls and the Mt-DNA copy number may be related to disease prognosis.

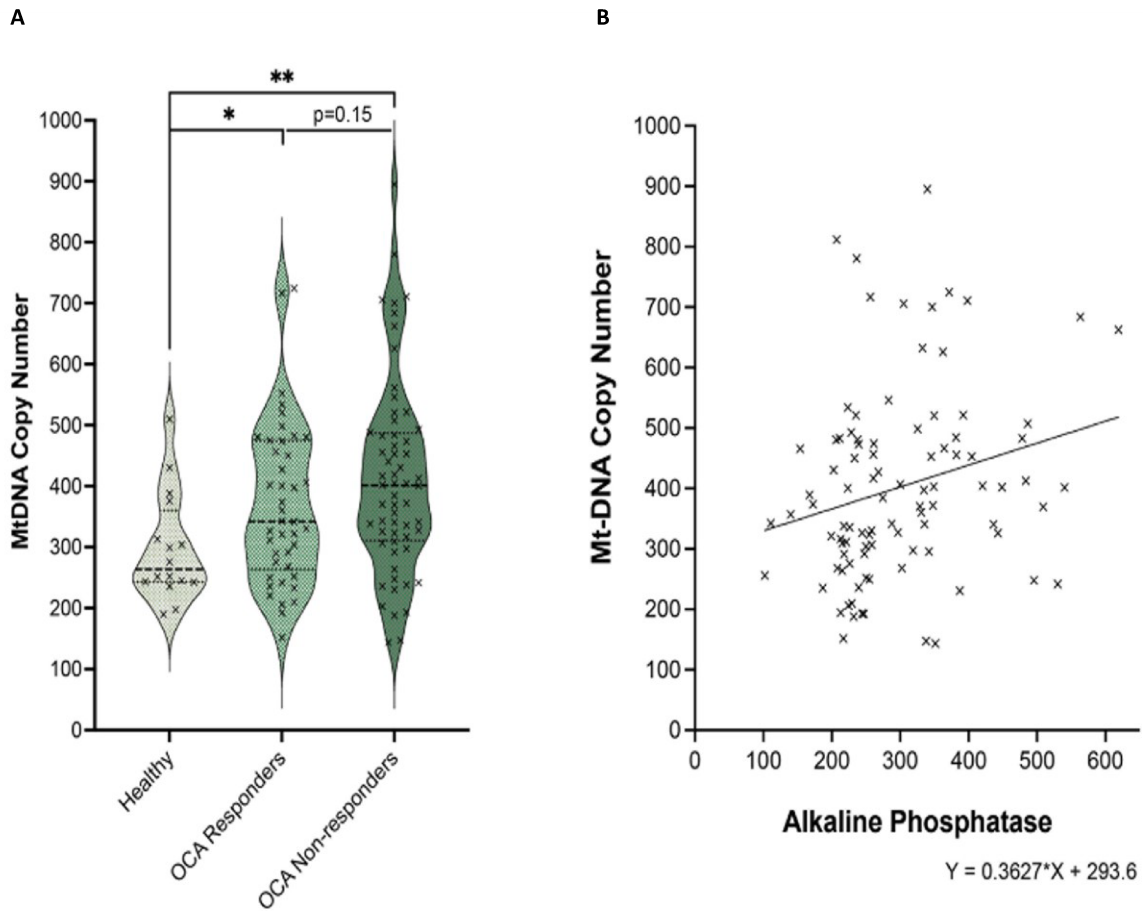


**Figure 13. Mitochondrial DNA copy number is increased in PBC peripheral blood**

(A) The violin plot showing the gradient increases of Mt-DNA copy number in healthy controls (n=16), OCA responders (n=42), and OCA non-responders (n=60). \* means  $p < 0.05$ , and \*\* means  $p < 0.01$ . Each point represents a sample. The plot is shown as median and IQR (Two-tailed Mann-Whitney test). (B) The linear regression plot examines the relationship between ALP (x-axis) and Mt-DNA copy number (y-axis). Each data point represents a value of a sample (n=95). The regression line, represented by the equation  $y = 0.3627X + 293.6$ , best fits the data points, indicating that Mt-DNA copy number is positively linear related with ALP.

### 3.6 Elevated mitochondrial membrane potential in PBC PBMC

The mitochondrial membrane potential ( $\Delta\Psi_m$ ) is the electrical potential difference across the inner mitochondrial membrane, which is crucial for various mitochondrial functions, including ATP production via oxidative phosphorylation. It reflects the health and functional state of the mitochondria. Abnormally high  $\Delta\Psi_m$  and low  $\Delta\Psi_m$  may indicate mitochondrial dysfunction. Tetramethyl rhodamine methyl ester (TMRM) is a fluorescent dye used to assess mitochondrial membrane potential. TMRM is a cationic, lipophilic compound that accumulates in the mitochondria in a potential-dependent manner. The more polarized (i.e., more negative inside) the mitochondrial membrane, the more TMRM is taken up by the mitochondria, leading to stronger fluorescence.

In order to evaluate  $\Delta\Psi_m$  of PBC and other control PBMC, MitoProbe™ TMRM signal was assessed by flow cytometric analysis. Healthy (n=8), PBC (n=9), and NASH (n=8) PBMC were incubated with viability stain and TMRM. Each sample had a CCCP control for the induction of mitochondrial membrane depolarization. All the CCCP promoted mitochondria uncoupling and reduce the TMRM signaling. The lymphocytes were gated first, then single cells were chosen. Live cells were gated to measure the median of fluorescence intensity (MFI) of the TMRM stain which were shown in Figure 14. The MFI of TMRM were extremely high in PBC and NASH compared to healthy controls, which indicated that some of PBMC of PBC and NASH had hyperpolarization of their mitochondria. Hyperpolarized mitochondria might affect the cellular functions of immune cells such as activation, proliferation, and cytokine production. This could lead to dysregulated immune responses or chronic inflammation.

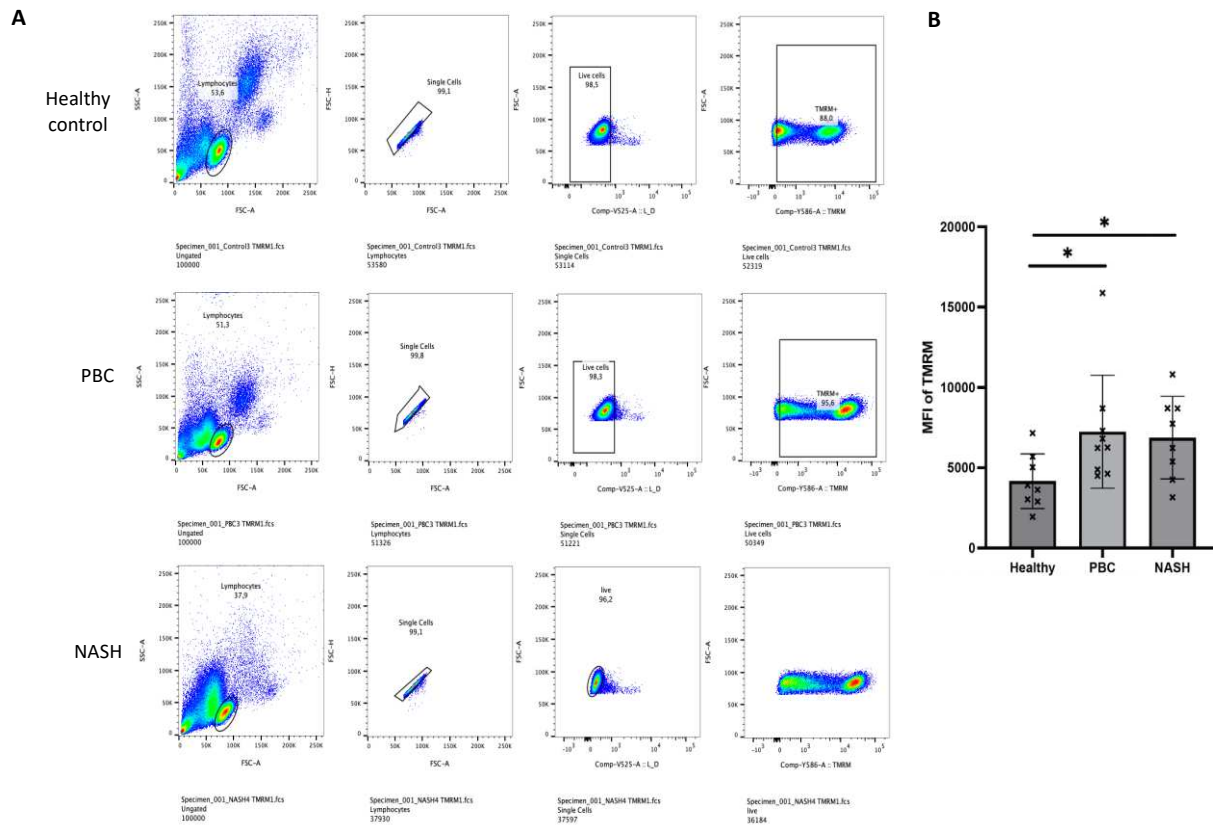


**Figure 14. Flow analysis of mitochondrial membrane potential in PBC PBMC**

(A) Flow cytometry gating strategies are shown. All single viable lymphocytes were gated. Gated percentages (%) indicate the frequency of targeted population. The median of fluorescence intensities (MFI) of TMRM was calculated by Flowjo. (B) Shows the MFI of TMRM of live lymphocytes population in healthy (n=8), PBC (n=9), and NASH (n=8). Each point represents a sample. The plot is shown as median and IQR, \* p < 0.05.

### 3.7 Increased AMA reactivity in PBC PBMC

The mitochondrial autoantigen expression in PBMC of PBC (n=3), healthy controls (n=3), and NASH (n=3) were evaluated by IF. We found that some PBMC in PBC had stronger AMA reactivities than the other cells, which illustrated some PBMC in PBC had increased expression of mitochondrial autoantigen (Figure 15A). The fluorescence intensity of PDC-E2 in PBC was almost double compared to healthy controls, and higher than NASH as well (Figure 15B).

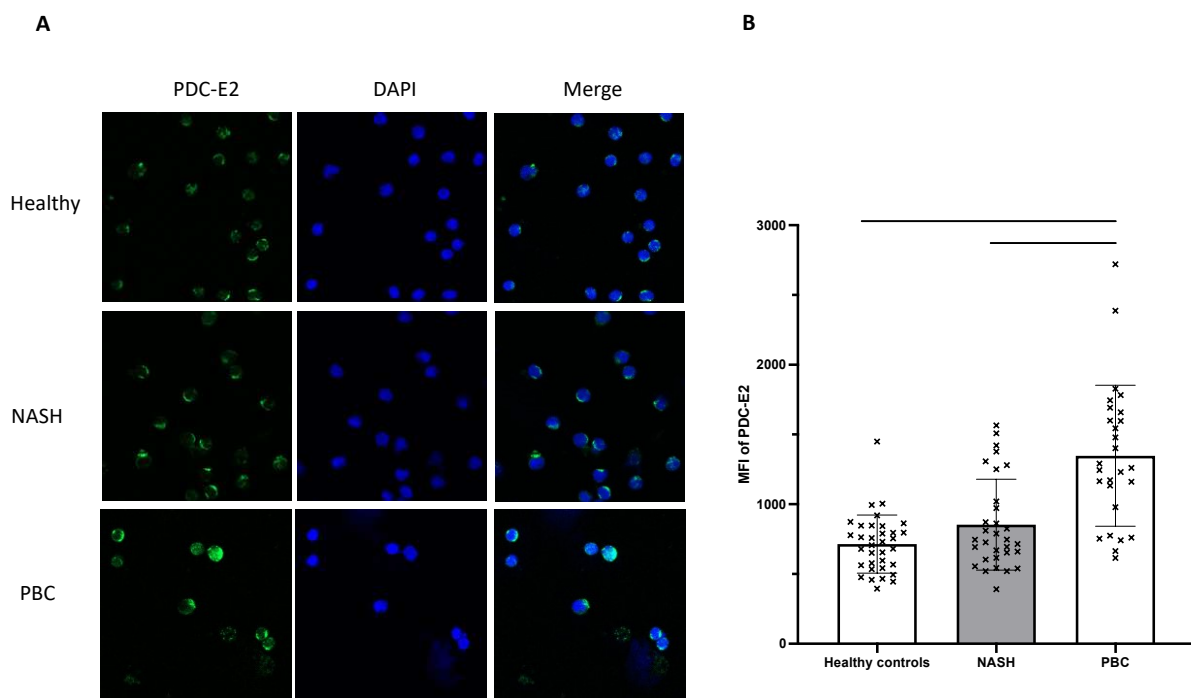


**Figure 15. Increased AMA reactivity in PBMC of patients with PBC**

(A) Representative photomicrographs of evaluation of AMA reactivity in PBMC of healthy, NASH, and PBC by immunofluorescence (IF) with AMA against PDC-E2 (green), and DAPI (blue). The images were performed using a Zeiss LSM-710. Original magnification: x 400, zoom x2. (B) Shows the fluorescence intensities of PDC-E2 in PBMC of healthy (n=34), PBC (n=27),

and NASH (n=31). The mean of fluorescence intensities of PDC-E2 per cell was calculated by ZEN. Each point represents a cell. The plot is shown as median and IQR, \*\*\*\*p < 0.0001.

### **3.8 PBMC with hyperpolarized mitochondria had more AMA reactivities**

As we do not know the mechanism and the consequences of hyperpolarization of mitochondria in PBC PBMC, we were interested to furtherly compare whether the mitochondrial autoantigen expression was different in PBMC with hyperpolarized mitochondria and PBMC without hyperpolarized mitochondria. TMRM-High PBMC and TMRM-Low PBMC were sorted by cell sorter Sony MA900 after staining by MitoProbe™ TMRM. Immunocytochemistry of AMA and DAPI was performed on these sorted cells after fixation directly following FACS. The median of fluorescence intensity (MFI) of AMA was measured for each cell. The TMRM-High PBMC had more AMA reactivities measured than TMRM-Low PBMC ( $p < 0.0001$ ). (Figure 16). This indicated that PBMC with hyperpolarized mitochondria may have more expression of mitochondrial autoantigen.

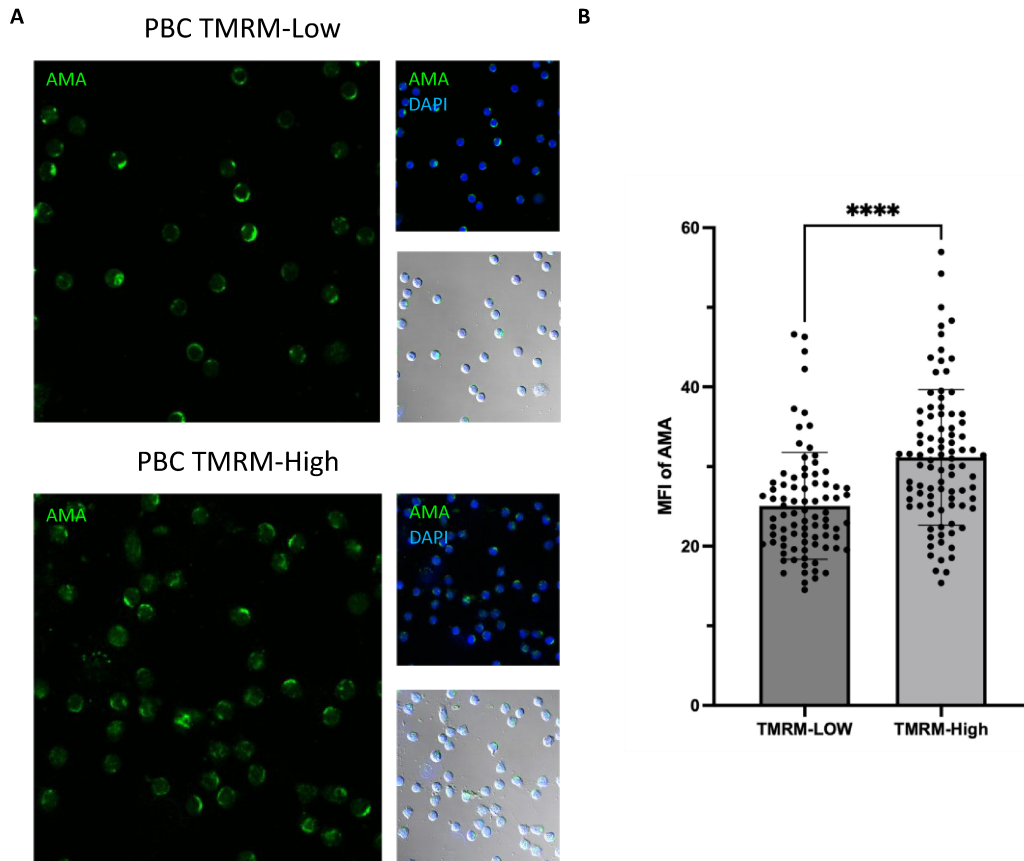


**Figure 16. Sorted PBMC of PBC with high TMRM have more AMA reactivity**

(A) Representative photomicrographs of sorted TMRM-High PBMC and TMRM-low PBMC of PBC stained by immunofluorescence (IF) with AMA against PDC-E2 (green), and DAPI (blue). The images were performed using a Zeiss LSM-710. Original magnification: x 400. (B) Shows the comparison of AMA reactivity in TMRM-High PBMC (n=84) and TMRM-low PBMC (n=91). The median of fluorescence intensities (MFI) of AMA reactivity per cell was calculated by ZEN. Each point represents a cell. The plot is shown as median and SD, \*\*\*\* p < 0.0001.

## **Chapter 4: Discussion**

### **4.1 Introduction**

In the present study, we investigated the one of the possible mechanisms of metabolic remodeling in cholangiocytes of patients with PBC. We found only specific cells in the biliary epithelium of PBC were characterized with activated HIF1  $\alpha$  signaling, but not in other liver cirrhosis. We also found the peripheral blood of PBC showed a systemic increased glycolytic metabolism phenotype with an upregulated mitochondrial encoded ETC and OXPHOS genes expression and a downregulated nuclear encoded genes expression. These inconsistent changes of gene expression were supported by increased MT-DNA replication and dysfunctional hyperpolarized mitochondria in PBC peripheral blood. Finally, the overexpression of mitochondrial autoantigen was associated with hyperpolarized mitochondria in PBMC of patients with PBC. Therefore, mitochondrial dysfunction characterized by hyperpolarized mitochondria induces compensated mitochondrial biogenesis which drives the overexpression of mitochondrial autoantigen in PBMC of PBC.

### **4.2 HIF-1 $\alpha$ signaling activation**

We showed that BECs with activated HIF1 $\alpha$  were in injured interlobular bile ducts, and the morphology of those cells' nuclei changed. A normal small cholangiocyte is cuboidal with a high nucleus/ cytoplasm ratio (68, 69). Those cells' nuclei had condensed and their cell size has shrunk, and some cells that had double nuclei expressed HIF-1 $\alpha$  in their nuclei. All of these changes illustrated cellular stress, or injury, or apoptosis. Of note was that HIF-1 $\alpha$  protects against oxidative stress by switching energy production from oxidative phosphorylation to glycolysis (70). For

instance, HIF-1 represses mitochondrial respiration and electron transfer chain activity by activating transcription ISCU1/2 and NDUFA4L2, thereby decreasing Complex I of ETC activity (71). HIF-1 $\alpha$  mediates a transition from oxidative to glycolytic metabolism through its regulation of many factors, such as PDK1, LDHA, BNIP3, and BNIP3L. PDK1 encodes pyruvate dehydrogenase (PDH) kinase 1, which phosphorylates and inactivates PDH, thereby inhibiting the conversion of pyruvate to acetyl coenzyme A for entry into the tricarboxylic acid cycle (72).

HIF-1 $\alpha$  activation in specific cells may contribute to ongoing cellular senescence in small bile ducts in PBC. Cellular senescence, defined by the cell cycle being arrested at the G1 phase, is triggered by several mechanisms including telomere shortening, DNA-damage, oxidative stress, and chronic inflammation (73). Biliary cellular senescence with telomere shortening and an accumulation of DNA damage was reported in damaged small bile ducts in PBC.  $\gamma$ H2AX-DNA-damage-foci were detected and increased the expression of p16<sup>INK4a</sup> and p21<sup>WAF1/Cip1</sup> which were assessed in the damaged bile ducts (74). The extent of senescent BECs was strongly correlated with the stage and activity of PBC, and the expression of p16<sup>INK4a</sup> in bile ductulus was correlated with the insufficient response to UDCA (75). Apoptosis resistance and hypersecretion of proinflammatory and profibrotic molecules are also hallmarks of cellular senescence. In senescent cells, apoptosis resistance is acquired by suppressing pro-apoptotic signaling and increasing senescent cell anti-apoptotic pathways (SCAPs). The key molecules of these anti-apoptotic pathways are the BCL-2 family members, including BCL-xL, and the HIF-1 $\alpha$ , PI3-kinase, and p21-related pathways (76).

Another hypothesis is that these double-nuclei HIF-1 $\alpha$  activated cells were cholangiocytes invaded by CD8<sup>+</sup> T cell. Cytotoxic T cells infiltrating around damaged small bile ducts were highly represented in PBC. Current studies found that CD8<sup>+</sup> T cells invaded BEC in PBC and this invasion was positively correlated with BEC injury and proliferation (77, 78). Expression of E-cadherin by CD8<sup>+</sup> T cells promotes their invasion into BEC (77). Interestingly, HIF-1 $\alpha$  was associated with CD8<sup>+</sup> T cell migration and effector functions in a tumor microenvironment (79). Therefore, HIF-1 $\alpha$  activation may have a role in cytotoxic T cell invasion of BEC.

Importantly, many studies have found a modulation of HIF-1 $\alpha$  by different types of viruses (80, 81). For instance, human immunodeficiency virus (HIV) is a retrovirus inducing cell death of CD4<sup>+</sup> T cells by infection. The viral protein Vpr enhances the expression of HIF-1 $\alpha$  by triggering cellular oxidative stress, leading to the accumulation of HIF-1 $\alpha$  protein, which in turn stimulates viral gene transcription (82, 83). Research indicates that cytosolic double-stranded DNA, produced during the HIV replication cycle in CD4<sup>+</sup> T cells, triggers mitochondrial ROS-dependent stabilization of HIF-1 $\alpha$ , thereby enhancing viral replication. The stabilization of HIF-1 $\alpha$  further promotes the release of extracellular vesicles, which, in turn, stimulate bystander CD4<sup>+</sup> T cells to secrete IFN- $\gamma$  and bystander macrophages to secrete IL-6 and IL-1 $\beta$  (84). Therefore, the HBRV infection of cholangiocytes may modulate the HIF-1 $\alpha$  inducing viral replication in bile ducts.

### **4.3 Mitochondrial phenotype in PBMC**

PBC predominantly occurs in females and AMA is a significant biomarker, so it is highly likely that the mitochondrial phenotype plays a crucial role in PBC pathogenesis. In mammals,

mitochondria are maternally inherited. HBRV may be transmitted through breastfeeding, spreading between the mammary glands and salivary glands as MMTV. Our previous studies have found that betaretrovirus infection could trigger the mitochondrial autoantigen overexpression in cholangiocytes. We also found that the metabolism of small cholangiocytes shifted to aerobic glycolysis, mitochondrial  $\Delta\Psi_m$  was elevated and Mt-DNA replication was increased. Thus, we hypothesized the same metabolic changes and mitochondrial features should be detected in lymphocytes if the viral infection induces this phenotype as HBRV likely would be able to infect both lymphocytes and cholangiocytes.

Therefore, we investigated the gene expression of metabolic pathways and bioenergetic pathways using whole blood RNA-seq data from PBC patients and healthy controls and found upregulated expression of glycolytic genes and opposite changes of MT-genes expression and NC-genes expression of ECT and OXPHOS. Maintaining functional OXPHOS requires for assembly of all the complexes subunits together, but how that assembly is regulated remains a mystery. The mitochondrial encoded OXPHOS proteins levels are regulated by translation, rather than by transcription in *saccharomyces cerevisiae* (85). A recent study identified a Mitochondrial Regulatory Hub for a respiratory assembly platform synchronized with Complex IV and ATP synthase biogenesis in yeast by Mra1 degradation (86). This evidence allows the possibility of opposite transcriptional changes in MT-genes and NC-genes. The increased Mt-DNA replication in PBC PBMC addressed subsequently agrees with the upregulated MT-genes transcription.

To further evaluate mitochondrial function, we used flow cytometry elevated  $\Delta\Psi_m$  and found that PBMC from PBC and NASH patients exhibit higher  $\Delta\Psi_m$  compared to healthy controls. From a

mechanism aspect, mitochondrial hyperpolarization (MHP) occurs when Complex IV is uncoupled from ATP synthesis and protons continue to be pumped into the intermembrane space, but are not used efficiently for ATP production. Chronic Complex I inhibition induces a proton-based  $\Delta\Psi_m$  hyperpolarization in HEK293 cells (87). MHP plays an important role in regulating T-cell activation and proliferation, and selection of the cell death pathway depends on the production of reactive oxygen species (ROS) (88). A previous study identified that T cell mitochondria responded to T-cell receptor (TCR) stimulation by increasing mass,  $\Delta\Psi_m$ , and ROS generation (89). Interestingly, betaretrovirus has a superantigen, the most variable region in the genome, which is efficiently stimulate T-cells via the crosslinking of TCR and MHC II molecules to enable viral replication within dividing cells (90, 91). Therefore, the MHP of PBC PBMC may be related to the HBRV infection.

We also found that PBC PBMC with MHP have an overexpression of mitochondrial autoantigen, but no AMA reactivity was found while the similar MHP was observed in NASH PBMC. Therefore, NASH works as a comparison to show that the increased MHP observed in NASH PBMC may be related to mitochondrial dysfunction. Mitochondrial dysfunction has been reported in hepatocytes and PBMC of NASH (92, 93). The mitochondrial dysfunction in hepatocytes can result in an inflammatory response due to the oxidative damage, which will release many proinflammatory cytokines such as IL-1, IL-6 and TNF- $\alpha$ . Lymphocytes will be activated by those cytokines, and will exhibit a high  $\Delta\Psi_m$  to meet their increased energy demands for proliferation (92).

#### **4.4 Future directions and conclusion**

To understand which type of cells in small bile ducts have HIF-1 $\alpha$  activation, we should use the different cell markers of lymphocytes, cholangiocytes, and progenitor cells. Finding HBRV antibody reactivities in those cells would add a piece of the puzzle to implicate a role for viral infection. Evaluating markers of apoptosis and senescence in these cells is also important for understanding the cell's state. A concern that cannot be ignored is the algorithm of our bioinformatic analysis may amplify the degree of change. Therefore, evaluating the functionality of Complex I - II and ATP synthase and the activity of some crucial enzymes in ECT will help us to understand the altered mitochondrial changes. Then, mitochondrial transcription factor A (TFAM) driving transcription and replication of mt-DNA should be investigated.

In summary, our results have shown that a systemic metabolic remodeling occurred in small cholangiocytes and PBMC in PBC including increased glycolytic enzymes and PDK which may be regulated by HIF1 $\alpha$  signaling activation. We also found altered mitochondrial function characterized by hyperpolarized mitochondria and increased mitochondrial DNA replication, which were associated with overexpression of PDC-E2.

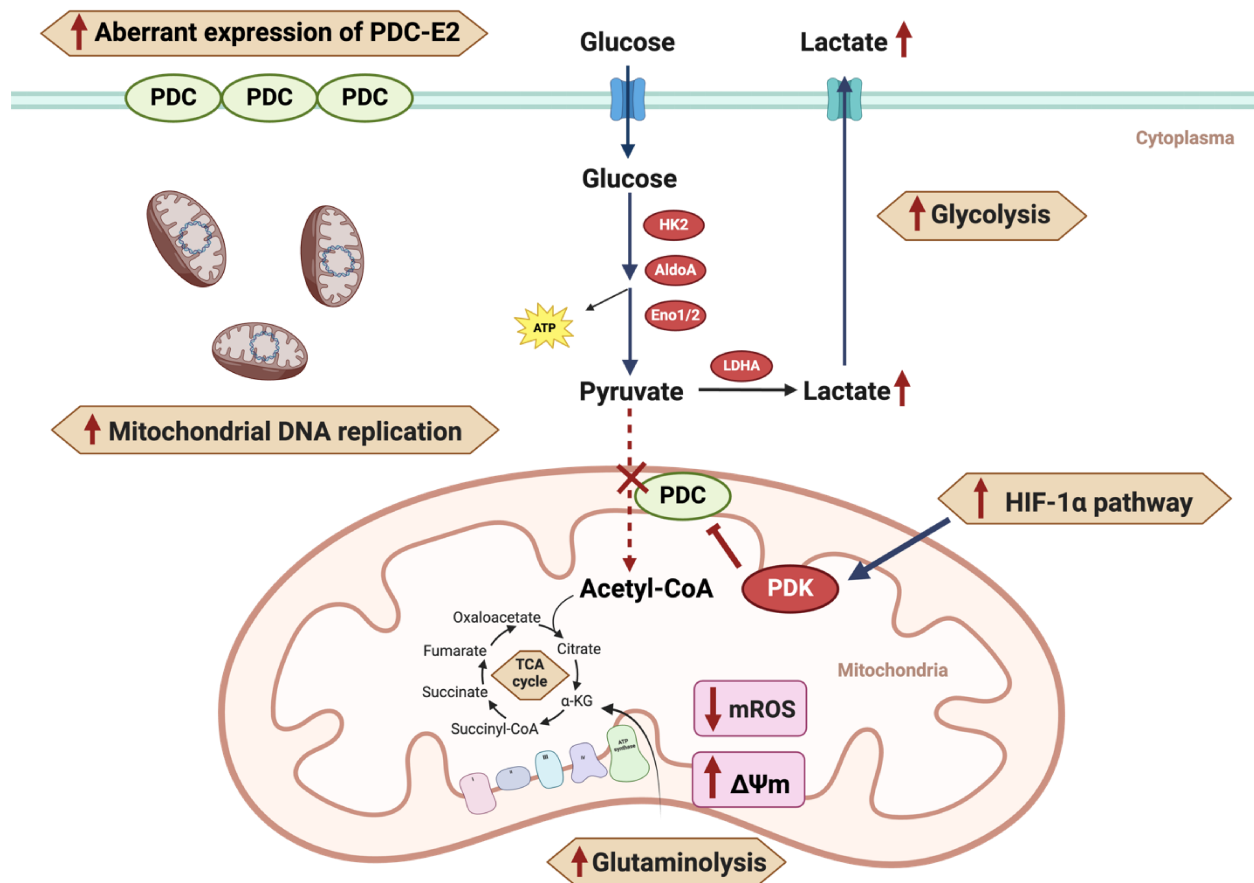


**Figure 17. The schematic of metabolism and abnormal mitochondrial signaling in cholangiocytes of patients with PBC**

Pyruvate dehydrogenase complex (PDC) E2 subunit which is one of the targets of antimitochondrial antibody (AMA) was observed on the cell surface of cholangiocytes of PBC. Pyruvate dehydrogenase kinase (PDK) activated by HIF-1α pathway inhibits PDC by phosphorylation, which triggers the metabolic remodeling in cholangiocytes by following pathways: 1) Pyruvate is converted to lactate instead of Acetyl-CoA, in addition with the result of upregulated glycolytic enzymes, inducing aerobic glycolysis; 2) Lacking substrates of TCA cycle alters the electron transport chain (ETC) efficiency resulting in hyperpolarized mitochondria,

diminished mitochondrial reactive oxygen species (mROS), and elevated mitochondrial DNA replication to compensate the lack of ATP production; 3) Cells also use glutaminolysis to produce substrates for TCA cycle with reduction in acetyl-CoA.

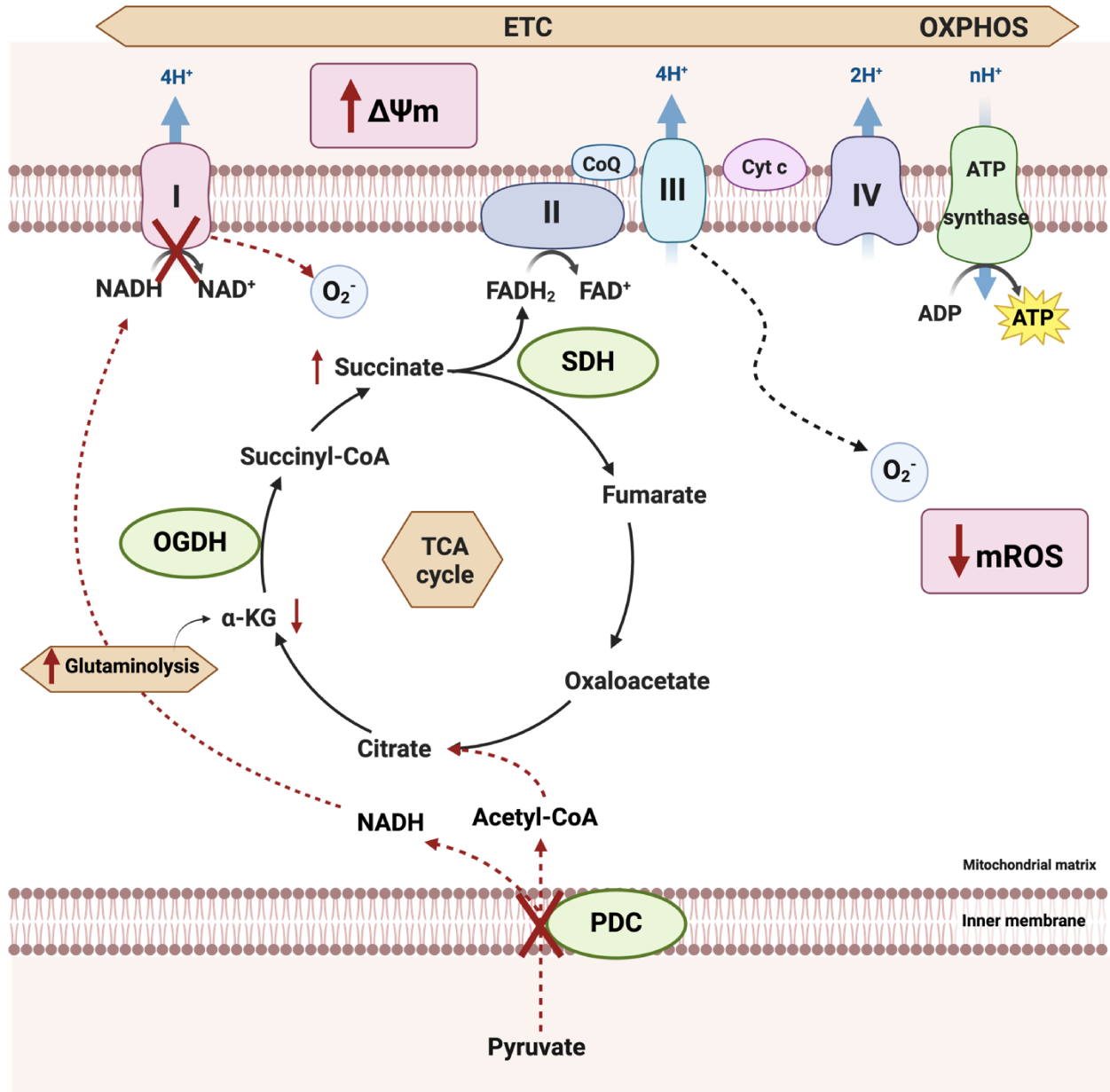


**Figure 18. The predicted schematic of mitochondrial energy production in cholangiocytes of patients with PBC**

The inhibition of Pyruvate dehydrogenase complex (PDC) reduces substrates for the TCA cycle and Complex I. However, the electron transport chain (ETC) continues to function with oxygen use because the mitochondrial membrane potential was high and mitochondrial reactive oxygen species (mROS) was low. With reduced Complex I activity, we predict a mechanism whereby Complex II increases activity to compensate the inhibition of Complex I to maintain the function of ETC. Because of lack of NADH and reduced mROS, we speculate that succinate dehydrogenase (SDH) activity will be increased, and glutaminolysis will provide increased succinate and FADH<sub>2</sub> as substrates of Complex II. In agreement, our metabolomic analysis of urine samples from patients with PBC and controls found an increased succinate and decreased  $\alpha$ -ketoglutarate in PBC.

## Bibliography

1. Carey EJ, Ali AH, Lindor KD. Primary biliary cirrhosis. *Lancet* 2015;386:1565-1575.
2. Talwalkar JA, Lindor KD. Primary biliary cirrhosis. *Lancet* 2003;362:53-61.
3. Trivella J, John BV, Levy C. Primary biliary cholangitis: Epidemiology, prognosis, and treatment. *Hepatol Commun* 2023;7.
4. Lleo A, Jepsen P, Morengi E, Carbone M, Moroni L, Battezzati PM, Podda M, et al. Evolving Trends in Female to Male Incidence and Male Mortality of Primary Biliary Cholangitis. *Sci Rep* 2016;6:25906.
5. John BV, Aitchison G, Schwartz KB, Khakoo NS, Dahman B, Deng Y, Goldberg D, et al. Male Sex Is Associated With Higher Rates of Liver-Related Mortality in Primary Biliary Cholangitis and Cirrhosis. *Hepatology* 2021;74:879-891.
6. Lv T, Chen S, Li M, Zhang D, Kong Y, Jia J. Regional variation and temporal trend of primary biliary cholangitis epidemiology: A systematic review and meta-analysis. *J Gastroenterol Hepatol* 2021;36:1423-1434.
7. Marschall HU, Henriksson I, Lindberg S, Soderdahl F, Thuresson M, Wahlin S, Ludvigsson JF. Incidence, prevalence, and outcome of primary biliary cholangitis in a nationwide Swedish population-based cohort. *Sci Rep* 2019;9:11525.
8. Prince MI, Chetwynd A, Craig WL, Metcalf JV, James OF. Asymptomatic primary biliary cirrhosis: clinical features, prognosis, and symptom progression in a large population based cohort. *Gut* 2004;53:865-870.
9. Onofrio FQ, Hirschfield GM, Gulamhusein AF. A Practical Review of Primary Biliary Cholangitis for the Gastroenterologist. *Gastroenterol Hepatol (N Y)* 2019;15:145-154.

10. Hirschfield GM, Dyson JK, Alexander GJM, Chapman MH, Collier J, Hubscher S, Patanwala I, et al. The British Society of Gastroenterology/UK-PBC primary biliary cholangitis treatment and management guidelines. *Gut* 2018;67:1568-1594.
11. Pares A, Caballeria L, Rodes J. Excellent long-term survival in patients with primary biliary cirrhosis and biochemical response to ursodeoxycholic Acid. *Gastroenterology* 2006;130:715-720.
12. Harms MH, van Buuren HR, Corpechot C, Thorburn D, Janssen HLA, Lindor KD, Hirschfield GM, et al. Ursodeoxycholic acid therapy and liver transplant-free survival in patients with primary biliary cholangitis. *J Hepatol* 2019;71:357-365.
13. Montano-Loza AJ, Corpechot C. Definition and Management of Patients With Primary Biliary Cholangitis and an Incomplete Response to Therapy. *Clin Gastroenterol Hepatol* 2021;19:2241-2251 e2241.
14. Yamagiwa S, Kamimura H, Takamura M, Aoyagi Y. Autoantibodies in primary biliary cirrhosis: recent progress in research on the pathogenetic and clinical significance. *World J Gastroenterol* 2014;20:2606-2612.
15. Montano-Loza AJ, Hansen BE, Corpechot C, Roccarina D, Thorburn D, Trivedi P, Hirschfield G, et al. Factors Associated With Recurrence of Primary Biliary Cholangitis After Liver Transplantation and Effects on Graft and Patient Survival. *Gastroenterology* 2019;156:94-107 e101.
16. Carbone M, Bufton S, Monaco A, Griffiths L, Jones DE, Neuberger JM. The effect of liver transplantation on fatigue in patients with primary biliary cirrhosis: a prospective study. *J Hepatol* 2013;59:490-494.

17. Lynch EN, Campani C, Innocenti T, Dragoni G, Biagini MR, Forte P, Galli A. Understanding fatigue in primary biliary cholangitis: From pathophysiology to treatment perspectives. *World J Hepatol* 2022;14:1111-1119.
18. Jopson L, Jones DE. Fatigue in Primary Biliary Cirrhosis: Prevalence, Pathogenesis and Management. *Dig Dis* 2015;33 Suppl 2:109-114.
19. Surh CD, Coppel R, Gershwin ME. Structural requirement for autoreactivity on human pyruvate dehydrogenase-E2, the major autoantigen of primary biliary cirrhosis. Implication for a conformational autoepitope. *J Immunol* 1990;144:3367-3374.
20. Fregeau DR, Davis PA, Danner DJ, Ansari A, Coppel RL, Dickson ER, Gershwin ME. Antimitochondrial antibodies of primary biliary cirrhosis recognize dihydrolipoamide acyltransferase and inhibit enzyme function of the branched chain alpha-ketoacid dehydrogenase complex. *J Immunol* 1989;142:3815-3820.
21. Moteki S, Leung PS, Dickson ER, Van Thiel DH, Galperin C, Buch T, Alarcon-Segovia D, et al. Epitope mapping and reactivity of autoantibodies to the E2 component of 2-oxoglutarate dehydrogenase complex in primary biliary cirrhosis using recombinant 2-oxoglutarate dehydrogenase complex. *Hepatology* 1994;23:436-444.
22. Patel MS, Nemeria NS, Furey W, Jordan F. The pyruvate dehydrogenase complexes: structure-based function and regulation. *J Biol Chem* 2014;289:16615-16623.
23. Qi F, Pradhan RK, Dash RK, Beard DA. Detailed kinetics and regulation of mammalian 2-oxoglutarate dehydrogenase. *BMC Biochem* 2011;12:53.
24. Dimou A, Tsimihodimos V, Bairaktari E. The Critical Role of the Branched Chain Amino Acids (BCAAs) Catabolism-Regulating Enzymes, Branched-Chain Aminotransferase (BCAT) and

Branched-Chain alpha-Keto Acid Dehydrogenase (BCKD), in Human Pathophysiology. *Int J Mol Sci* 2022;23.

25. Courvalin JC, Lassoued K, Bartnik E, Blobel G, Wozniak RW. The 210-kD nuclear envelope polypeptide recognized by human autoantibodies in primary biliary cirrhosis is the major glycoprotein of the nuclear pore. *J Clin Invest* 1990;86:279-285.

26. Szostecki C, Will H, Netter HJ, Guldner HH. Autoantibodies to the nuclear Sp100 protein in primary biliary cirrhosis and associated diseases: epitope specificity and immunoglobulin class distribution. *Scand J Immunol* 1992;36:555-564.

27. Comby E, Tanaff P, Mariotte D, Costentin-Pignol V, Marcelli C, Ballet JJ. Evolution of antinuclear antibodies and clinical patterns in patients with active rheumatoid arthritis with longterm infliximab therapy. *J Rheumatol* 2006;33:24-30.

28. Novak S. [Clinical significance of antinuclear antibodies and other serological abnormalities in systemic lupus erythematosus (SLE)]. *Reumatizam* 2009;56:22-25.

29. Zhang WC, Zhao FR, Chen J, Chen WX. Meta-analysis: diagnostic accuracy of antinuclear antibodies, smooth muscle antibodies and antibodies to a soluble liver antigen/liver pancreas in autoimmune hepatitis. *PLoS One* 2014;9:e92267.

30. Garcia MJ, Rodriguez-Duque JC, Pascual M, Rivas C, Castro B, Raso S, Lopez-Hoyos M, et al. Prevalence of antinuclear antibodies in inflammatory bowel disease and seroconversion after biological therapy. *Therap Adv Gastroenterol* 2022;15:17562848221077837.

31. Van de Water J, Ansari A, Prindiville T, Coppel RL, Ricalton N, Kotzin BL, Liu S, et al. Heterogeneity of autoreactive T cell clones specific for the E2 component of the pyruvate dehydrogenase complex in primary biliary cirrhosis. *J Exp Med* 1995;181:723-733.

32. Shimoda S, Nakamura M, Shigematsu H, Tanimoto H, Gushima T, Gershwin ME, Ishibashi H. Mimicry peptides of human PDC-E2 163-176 peptide, the immunodominant T-cell epitope of primary biliary cirrhosis. *Hepatology* 2000;31:1212-1216.
33. Kita H, Matsumura S, He XS, Ansari AA, Lian ZX, Van de Water J, Coppel RL, et al. Quantitative and functional analysis of PDC-E2-specific autoreactive cytotoxic T lymphocytes in primary biliary cirrhosis. *J Clin Invest* 2002;109:1231-1240.
34. Duan W, Chen S, Li S, Lv T, Li B, Wang X, Wang Y, et al. The future risk of primary biliary cholangitis (PBC) is low among patients with incidental anti-mitochondrial antibodies but without baseline PBC. *Hepatol Commun* 2022;6:3112-3119.
35. Beuers U, Hohenester S. Fatigue in Primary Biliary Cholangitis: No Place for Rituximab. *Hepatology* 2019;70:1503-1505.
36. Gershwin ME, Selmi C, Worman HJ, Gold EB, Watnik M, Utts J, Lindor KD, et al. Risk factors and comorbidities in primary biliary cirrhosis: a controlled interview-based study of 1032 patients. *Hepatology* 2005;42:1194-1202.
37. Fussey SP, Ali ST, Guest JR, James OF, Bassendine MF, Yeaman SJ. Reactivity of primary biliary cirrhosis sera with *Escherichia coli* dihydrolipoamide acetyltransferase (E2p): characterization of the main immunogenic region. *Proc Natl Acad Sci U S A* 1990;87:3987-3991.
38. Xu L, Sakalian M, Shen Z, Loss G, Neuberger J, Mason A. Cloning the human betaretrovirus proviral genome from patients with primary biliary cirrhosis. *Hepatology* 2004;39:151-156.
39. Xu L, Shen Z, Guo L, Fodera B, Keogh A, Joplin R, O'Donnell B, et al. Does a betaretrovirus infection trigger primary biliary cirrhosis? *Proc Natl Acad Sci U S A* 2003;100:8454-8459.

40. Selmi C, Mayo MJ, Bach N, Ishibashi H, Invernizzi P, Gish RG, Gordon SC, et al. Primary biliary cirrhosis in monozygotic and dizygotic twins: genetics, epigenetics, and environment. *Gastroenterology* 2004;127:485-492.
41. Ornolfsson KT, Olafsson S, Bergmann OM, Gershwin ME, Bjornsson ES. Using the Icelandic genealogical database to define the familial risk of primary biliary cholangitis. *Hepatology* 2018;68:166-171.
42. Mulinacci G, Palermo A, Gerussi A, Asselta R, Gershwin ME, Invernizzi P. New insights on the role of human leukocyte antigen complex in primary biliary cholangitis. *Front Immunol* 2022;13:975115.
43. Invernizzi P, Ransom M, Raychaudhuri S, Kosoy R, Lleo A, Shigeta R, Franke A, et al. Classical HLA-DRB1 and DPB1 alleles account for HLA associations with primary biliary cirrhosis. *Genes Immun* 2012;13:461-468.
44. Li M, Zheng H, Tian QB, Rui MN, Liu DW. HLA-DR polymorphism and primary biliary cirrhosis: evidence from a meta-analysis. *Arch Med Res* 2014;45:270-279.
45. Darlay R, Ayers KL, Mells GF, Hall LS, Liu JZ, Almarri MA, Alexander GJ, et al. Amino acid residues in five separate HLA genes can explain most of the known associations between the MHC and primary biliary cholangitis. *PLoS Genet* 2018;14:e1007833.
46. Qiu F, Tang R, Zuo X, Shi X, Wei Y, Zheng X, Dai Y, et al. A genome-wide association study identifies six novel risk loci for primary biliary cholangitis. *Nat Commun* 2017;8:14828.
47. Hitomi Y, Nakamura M. The Genetics of Primary Biliary Cholangitis: A GWAS and Post-GWAS Update. *Genes (Basel)* 2023;14.
48. Joshita S, Umemura T, Tanaka E, Ota M. Genetics and epigenetics in the pathogenesis of primary biliary cholangitis. *Clin J Gastroenterol* 2018;11:11-18.

49. Gerussi A, Carbone M, Corpechot C, Schramm C, Asselta R, Invernizzi P. The genetic architecture of primary biliary cholangitis. *Eur J Med Genet* 2021;64:104292.
50. Sun L, He C, Nair L, Yeung J, Egwuagu CE. Interleukin 12 (IL-12) family cytokines: Role in immune pathogenesis and treatment of CNS autoimmune disease. *Cytokine* 2015;75:249-255.
51. Liaskou E, Patel SR, Webb G, Bagkou Dimakou D, Akiror S, Krishna M, Mells G, et al. Increased sensitivity of Treg cells from patients with PBC to low dose IL-12 drives their differentiation into IFN-gamma secreting cells. *J Autoimmun* 2018;94:143-155.
52. Tsuneyama K, Baba H, Morimoto Y, Tsunematsu T, Ogawa H. Primary Biliary Cholangitis: Its Pathological Characteristics and Immunopathological Mechanisms. *J Med Invest* 2017;64:7-13.
53. Purohit T, Cappell MS. Primary biliary cirrhosis: Pathophysiology, clinical presentation and therapy. *World J Hepatol* 2015;7:926-941.
54. Tsuneyama K, Van de Water J, Leung PS, Cha S, Nakanuma Y, Kaplan M, De Lellis R, et al. Abnormal expression of the E2 component of the pyruvate dehydrogenase complex on the luminal surface of biliary epithelium occurs before major histocompatibility complex class II and BB1/B7 expression. *Hepatology* 1995;21:1031-1037.
55. Shimoda S, Hisamoto S, Harada K, Iwasaka S, Chong Y, Nakamura M, Bekki Y, et al. Natural killer cells regulate T cell immune responses in primary biliary cirrhosis. *Hepatology* 2015;62:1817-1827.
56. Prieto J, Banales JM, Medina JF. Primary biliary cholangitis: pathogenic mechanisms. *Curr Opin Gastroenterol* 2021;37:91-98.

57. Van de Water J, Gerson LB, Ferrell LD, Lake JR, Coppel RL, Batts KP, Wiesner RH, et al. Immunohistochemical evidence of disease recurrence after liver transplantation for primary biliary cirrhosis. *Hepatology* 1994;24:1079-1084.
58. Wang GL, Semenza GL. General involvement of hypoxia-inducible factor 1 in transcriptional response to hypoxia. *Proc Natl Acad Sci U S A* 1993;90:4304-4308.
59. Wang GL, Jiang BH, Rue EA, Semenza GL. Hypoxia-inducible factor 1 is a basic-helix-loop-helix-PAS heterodimer regulated by cellular O<sub>2</sub> tension. *Proc Natl Acad Sci U S A* 1995;92:5510-5514.
60. Hayashi Y, Yokota A, Harada H, Huang G. Hypoxia/pseudohypoxia-mediated activation of hypoxia-inducible factor-1alpha in cancer. *Cancer Sci* 2019;110:1510-1517.
61. Wilson GK, Tennant DA, McKeating JA. Hypoxia inducible factors in liver disease and hepatocellular carcinoma: current understanding and future directions. *J Hepatol* 2014;61:1397-1406.
62. Mohlin S, Wigerup C, Jogi A, Pahlman S. Hypoxia, pseudohypoxia and cellular differentiation. *Exp Cell Res* 2017;356:192-194.
63. Kluckova K, Tennant DA. Metabolic implications of hypoxia and pseudohypoxia in pheochromocytoma and paraganglioma. *Cell Tissue Res* 2018;372:367-378.
64. Grimolizzi F, Arranz L. Multiple faces of succinate beyond metabolism in blood. *Haematologica* 2018;103:1586-1592.
65. Burr SP, Costa AS, Grice GL, Timms RT, Lobb IT, Freisinger P, Dodd RB, et al. Mitochondrial Protein Lipoylation and the 2-Oxoglutarate Dehydrogenase Complex Controls HIF1alpha Stability in Aerobic Conditions. *Cell Metab* 2016;24:740-752.

66. Semenza GL. Hypoxia-inducible factors in physiology and medicine. *Cell* 2012;148:399-408.
67. Nevens F, Andreone P, Mazzella G, Strasser SI, Bowlus C, Invernizzi P, Drenth JP, et al. A Placebo-Controlled Trial of Obeticholic Acid in Primary Biliary Cholangitis. *N Engl J Med* 2016;375:631-643.
68. Benedetti A, Bassotti C, Rapino K, Marucci L, Jezequel AM. A morphometric study of the epithelium lining the rat intrahepatic biliary tree. *J Hepatol* 1994;24:335-342.
69. Lleo A, Maroni L, Glaser S, Alpini G, Marzioni M. Role of cholangiocytes in primary biliary cirrhosis. *Semin Liver Dis* 2014;34:273-284.
70. Semenza GL. Hypoxia-inducible factor 1: regulator of mitochondrial metabolism and mediator of ischemic preconditioning. *Biochim Biophys Acta* 2011;1813:1263-1268.
71. Chan SY, Zhang YY, Hemann C, Mahoney CE, Zweier JL, Loscalzo J. MicroRNA-210 controls mitochondrial metabolism during hypoxia by repressing the iron-sulfur cluster assembly proteins ISCU1/2. *Cell Metab* 2009;10:273-284.
72. Kim JW, Tchernyshyov I, Semenza GL, Dang CV. HIF-1-mediated expression of pyruvate dehydrogenase kinase: a metabolic switch required for cellular adaptation to hypoxia. *Cell Metab* 2006;3:177-185.
73. Calcinotto A, Kohli J, Zagato E, Pellegrini L, Demaria M, Alimonti A. Cellular Senescence: Aging, Cancer, and Injury. *Physiol Rev* 2019;99:1047-1078.
74. Sasaki M, Ikeda H, Yamaguchi J, Nakada S, Nakanuma Y. Telomere shortening in the damaged small bile ducts in primary biliary cirrhosis reflects ongoing cellular senescence. *Hepatology* 2008;48:186-195.

75. Sasaki M, Sato Y, Nakanuma Y. Increased p16(INK4a)-expressing senescent bile ductular cells are associated with inadequate response to ursodeoxycholic acid in primary biliary cholangitis. *J Autoimmun* 2020;107:102377.
76. Trussoni CE, O'Hara SP, LaRusso NF. Cellular senescence in the cholangiopathies: a driver of immunopathology and a novel therapeutic target. *Semin Immunopathol* 2022;44:527-544.
77. Davies SP, Ronca V, Wootton GE, Krajewska NM, Bozward AG, Fiancette R, Patten DA, et al. Expression of E-cadherin by CD8(+) T cells promotes their invasion into biliary epithelial cells. *Nat Commun* 2024;15:853.
78. Zhao SX, Li WC, Fu N, Zhou GD, Liu SH, Jiang LN, Zhang YG, et al. Emperipolesis mediated by CD8(+) T cells correlates with biliary epithelia cell injury in primary biliary cholangitis. *J Cell Mol Med* 2020;24:1268-1275.
79. Palazon A, Tyrakis PA, Macias D, Velica P, Rundqvist H, Fitzpatrick S, Vojnovic N, et al. An HIF-1alpha/VEGF-A Axis in Cytotoxic T Cells Regulates Tumor Progression. *Cancer Cell* 2017;32:669-683 e665.
80. Reyes A, Corrales N, Galvez NMS, Bueno SM, Kalergis AM, Gonzalez PA. Contribution of hypoxia inducible factor-1 during viral infections. *Virulence* 2020;11:1482-1500.
81. Reyes A, Duarte LF, Farias MA, Tognarelli E, Kalergis AM, Bueno SM, Gonzalez PA. Impact of Hypoxia over Human Viral Infections and Key Cellular Processes. *Int J Mol Sci* 2021;22.
82. Deshmane SL, Amini S, Sen S, Khalili K, Sawaya BE. Regulation of the HIV-1 promoter by HIF-1alpha and Vpr proteins. *Virology* 2011;8:477.
83. Deshmane SL, Mukerjee R, Fan S, Del Valle L, Michiels C, Sweet T, Rom I, et al. Activation of the oxidative stress pathway by HIV-1 Vpr leads to induction of hypoxia-inducible factor 1alpha expression. *J Biol Chem* 2009;284:11364-11373.

84. Duette G, Pereyra Gerber P, Rubione J, Perez PS, Landay AL, Crowe SM, Liao Z, et al. Induction of HIF-1alpha by HIV-1 Infection in CD4(+) T Cells Promotes Viral Replication and Drives Extracellular Vesicle-Mediated Inflammation. *mBio* 2018;9.
85. Kaur J, Datta K. IRC3 Regulates Mitochondrial Translation in Response to Metabolic Cues in *Saccharomyces cerevisiae*. *Mol Cell Biol* 2021;41:e0023321.
86. Moretti-Horten DN, Peselj C, Taskin AA, Myketin L, Schulte U, Einsle O, Drepper F, et al. Synchronized assembly of the oxidative phosphorylation system controls mitochondrial respiration in yeast. *Dev Cell* 2024;59:1043-1057 e1048.
87. Forkink M, Manjeri GR, Liemburg-Apers DC, Nibbeling E, Blanchard M, Wojtala A, Smeitink JA, et al. Mitochondrial hyperpolarization during chronic complex I inhibition is sustained by low activity of complex II, III, IV and V. *Biochim Biophys Acta* 2014;1837:1247-1256.
88. Chen J, Chernatynskaya AV, Li JW, Kimbrell MR, Cassidy RJ, Perry DJ, Muir AB, et al. T cells display mitochondria hyperpolarization in human type 1 diabetes. *Sci Rep* 2017;7:10835.
89. Nagy G, Koncz A, Perl A. T cell activation-induced mitochondrial hyperpolarization is mediated by Ca<sup>2+</sup>- and redox-dependent production of nitric oxide. *J Immunol* 2003;171:5188-5197.
90. Held W, Waanders GA, Shakhov AN, Scarpellino L, Acha-Orbea H, MacDonald HR. Superantigen-induced immune stimulation amplifies mouse mammary tumor virus infection and allows virus transmission. *Cell* 1993;74:529-540.
91. Weber GF, Abromson-Leeman S, Cantor H. A signaling pathway coupled to T cell receptor ligation by MMTV superantigen leading to transient activation and programmed cell death. *Immunity* 1995;2:363-372.

92. Garrafa E, Segala A, Vezzoli M, Bottani E, Zanini B, Vetturi A, Bracale R, et al. Mitochondrial Dysfunction in Peripheral Blood Mononuclear Cells as Novel Diagnostic Tools for Non-Alcoholic Fatty Liver Disease: Visualizing Relationships with Known and Potential Disease Biomarkers. *Diagnostics (Basel)* 2023;13.
93. Prasun P, Ginevic I, Oishi K. Mitochondrial dysfunction in nonalcoholic fatty liver disease and alcohol related liver disease. *Transl Gastroenterol Hepatol* 2021;6:4.
94. Filip Wysokinski, Characterization of the Mitochondrial Phenotype Associated with Primary Biliary Cholangitis (Master's thesis). University of Alberta 2017.